DEVELOPMENT OF MICRO-PATTERNED FILMS FOR OPTHTHALMIC DRUG DELIVERY

By

Mrunal Kamlesh Sakharkar

B.Tech. Pharmaceutical Sciences, Institute of Chemical Technology, 2017

Submitted to the Graduate Faculty of

School of Pharmacy in partial fulfillment

of the requirements for the degree of

Master of Science

University of Pittsburgh

2019

UNIVERSITY OF PITTSBURGH

SCHOOL OF PHARMACY

This thesis was presented

by

Mrunal Kamlesh Sakharkar

It was defended on

27th March 2019

and approved by

Lisa Rohan, Ph.D., Professor, Department of Pharmaceutical Sciences, School of Pharmacy

Song Li, Ph.D., Professor, Department of Pharmaceutical Sciences, School of Pharmacy

Thesis Advisor: Vinayak Sant, Ph.D., Assistant Professor, Department of Pharmaceutical Sciences, School of Pharmacy

DEVELOPMENT OF MICRO-PATTERNED FILMS FOR OPHTHALMIC DRUG DELIVERY

Mrunal Kamlesh Sakharkar, B.Tech.

University of Pittsburgh, 2019

ABSTRACT

Ocular inflammation is commonly associated with multiple eye disorders such as microbial infections, allergies and post-operative healing. Topical anti-inflammatory agents delivered via eye drops or ointments are commonly used for the management of inflammation. These treatment regimens involve high dosing frequency over prolonged periods depending on the severity of inflammation. Further, only 5% of administered drug may be available for action due to the physiological barriers of the eye and formulation losses. Collectively, this reduces patient compliance and causes irregularity in drug exposure. Therefore, there is a need for prolonged residence time of formulation in the eye to achieve sustained drug delivery. Mucoadhesive polymers and ocular inserts have been used for this purpose. Additionally, topographical features have been explored to enhance adhesion to mucosal surfaces. Taking inspiration from these approaches, we hypothesized that micropatterned polymeric films will prolong residence time by enhancing interactions with ocular mucosal surface and sustain the drug release.

We developed micropatterned films containing a hydrophobic drug, hydrocortisone (HCT) or a hydrophilic drug, olopatadine hydrochloride (OLO) using GRAS-compliant cellulose-based polymers and polylactic-co-glycolic acid (PLGA). Films with 100 μm sized square, triangle and circle micropatterns were manufactured and characterized for HCT / OLO release. We demonstrated an *in vitro* sustained release for up to 72 hours, for both HCT and OLO. The shape

of micropatterns did not impact drug release, however, PLGA and hydroxyethylcellulose impacted release of HCT and OLO, respectively. Tensile properties of films were dependent on the film composition and not micropatterns. A novel method to investigate the mucoadhesion potential of micropatterned films was developed. For cellulose and PLGA-based films, micropatterns did not improve adhesion to porcine intestinal tissue. Collectively, our results suggest that sustained release of anti-inflammatory drugs can be achieved by using cellulose and PLGA-based films and the presence of 100 μm sized micropatterns did not improve adhesion to mucosal surface. Further optimization of formulation and micropattern characteristics will be required to maximize sustained release and mucoadhesion in films, which can potentially be used for long-term delivery to the anterior region of the eye.

Keywords: Micropatterns, polymeric films, hydrocortisone, olopatadine hydrochloride, HPMC, HEC, HPC, PLGA, mucoadhesion

Table of Contents

List of Tables

List of Figures

Acknowledgements

I wish to express sincere gratitude towards my advisor Dr. Vinayak Sant for his constant motivation, guidance and support. His mentorship and perspective propelled me to learn new things and approach problems in a unique way. I sincerely thank Dr. Shilpa Sant for always being approachable, sharing her insights and helping me develop my soft skills.

I also wish to thank my past and current fellow lab members, Dr.Yingfei Xue, Akhil Patel, Vishal Rakshe, Urmi Chheda and Aishwarya Vasudevan for being the great colleagues they are. I wish to acknowledge and thank Prithivirajan Durairajan for his patience and help in training me. I express deep gratitude towards Dr. Lisa Rohan and her lab members for allowing me to access various instruments and training me for those. I would like to thank Dr. Robert Gibbs for providing access to the confocal microscope.

I wish to thank Dr. Maggie Folan, Lori Altenbaugh and Dolores Hornick for their help in various facets of my journey. I sincerely thank the faculty and fellow students of the School of Pharmacy at University of Pittsburgh.

I am immensely grateful for my parents and my brother, Shreekant, for always having faith in me and providing unconditional love and support throughout. Last, but not the least, I am thankful to my friend Rachana, and Dr. Prema Iyer for being my family away from home.

Abbreviations

DIC microscopy: Differential Interference Contrast microscopy

DSC: Differential Scanning Calorimetry

FDA: Food and Drug Administration

FITC: Fluorescein isothiocyanate

HCT: Hydrocortisone

HEC: Hydroxyethylcellulose

HPC: Hydroxypropylcellulose

HPMC: Hydroxypropylmethylcellulose

ICH: International Conference on Harmonization

MN: Microneedles

OLO: Olopatadine hydrochloride

PDMS: Polydimethylsiloxane

PEG: Polyethylene glycol

PLGA: Polylactic-co-glycolide acid

STF: Simulated Tear Fluid

UV: Ultraviolet

XRD: X-ray diffraction

1.0 Introduction

Visual impairment is one of the major concerns globally as it can have a negative impact on the day-to-day functioning of patients and exposes them to a higher risk of accidents, depression, social withdrawal and mortality [1]. At least 24 million Americans suffer from various eye-related conditions such as cataracts, glaucoma, age-related macular degeneration, dry eye syndrome and ocular manifestations of other chronic diseases [2]. In addition to the personal and social issues, management of these conditions involves a huge financial burden on the affected individuals [3]. To address these problems, extensive research is being conducted in ocular drug delivery to develop new therapeutic moieties and treatment regimens, and towards improving the efficiency of these intended therapies.

Ocular drug delivery remains a challenge in the treatment of local diseases of the eye and its comorbidities associated with other chronic conditions. The complex and sensitive nature of the organ imposes restrictions on xenobiotics and potential drug delivery systems used in the treatment. These hurdles are a result of the anatomical structure and physiological conditions of the eye. Therefore, there is a need to account for these hurdles when developing a platform for ocular drug delivery.

1.1 Anatomy and physiology of the eye

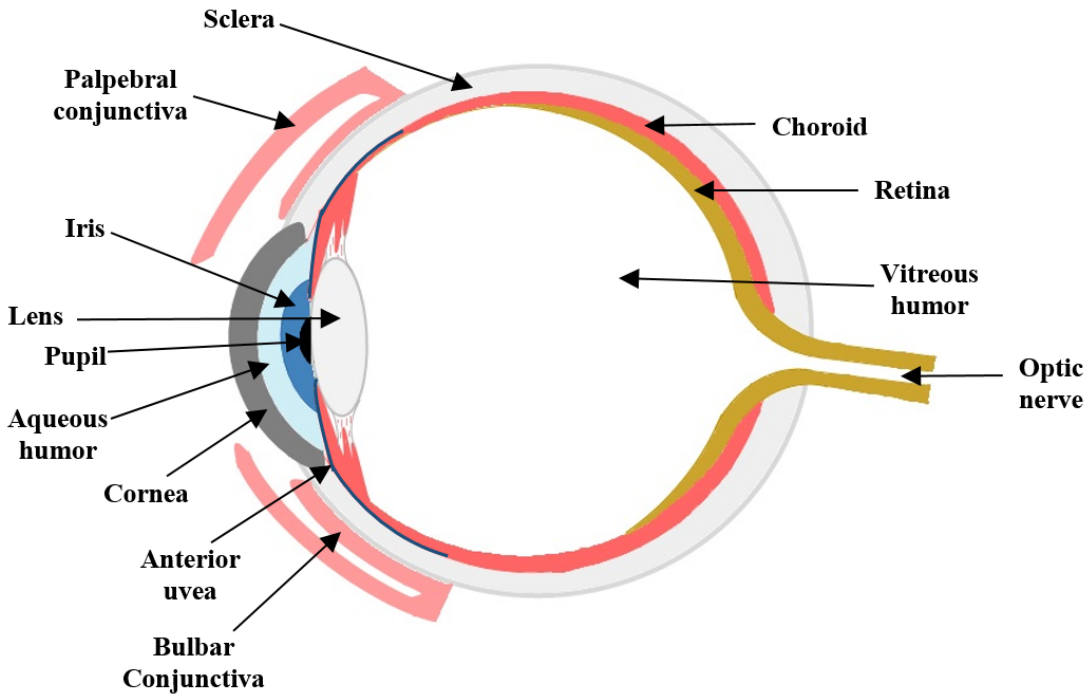

Figure 1: Schematic of the the eye

The eye can be broadly classified into two regions, the anterior and the posterior region. The anterior region comprises of the cornea, iris, pupil, sclera, anterior uvea etc. whereas the posterior region comprises of the vitreous humor, retina, choroid etc. (Figure 1). The cornea is the transparent and outermost layer which eventually merges into the sclera, the white of the eye. The sclera and eyelids are lined by a thin, vascularized tissue known as the conjunctiva. The surface of the eye, particularly the cornea, sclera and conjunctiva, are covered by a protective tear film. The tear film is typically a few microns in thickness and 7- 10 µL in volume with a turnover of 1-2 $\mu L min^{-1}$ [4-6]. It consists of a lipid layer, an aqueous layer and mucins. The surface glycocalyx of corneal epithelial cells and goblet cells in the conjunctiva is composed of transmembrane mucins,

which are also secreted into the tear film to achieve a mucin concentration of approximately 0.01% [7, 8]. The static anatomical barriers such as corneal epithelium, stroma and endothelium along with dynamic physiological barriers like blinking, tear turnover, nasolacrimal drainage, induced tear production, and conjunctival blood flow affect the local concentration and permeation of the drug [4, 9]. These anatomical and physiological barriers of the eye must be overcome by drug molecules to achieve desired local therapeutic concentrations.

The corneal epithelium is lipoidal in nature posing a resistance against the permeation of topically applied hydrophilic drugs. On the other hand, the stroma is a highly hydrated structure and poses a significant barrier to the permeation of lipophilic drug molecules [4]. High tear turnover and nasolacrimal drainage would remove the formulation from the ocular surface resulting in a contact time of less than 2 minutes [10]. In addition, blinking creates local shear forces which may impact the physical integrity of drug delivery system. Excessive conjunctival blood flow can cause significant drug loss in the systemic circulation, thereby lowering the ocular bioavailability [9].

However, in cases of conjunctivitis, corneal abrasion, microbial infection and post-operative inflammation, the conjunctiva is an attractive site of drug administration. The conjunctival surface area is 17 times the corneal area [11] allowing more drug to be absorbed per unit time. The amount of drug formulation delivered can be more and it can serve as a depot of drug when delivered in the conjunctival region.

In general, it can be summarized that the various barriers in the eye challenge the permeation of the drug but primarily, cause loss in the formulation available on the surface. To prevent these losses, there is a need to improve the residence time of a formulation in the eye, which can deliver the drug in a controlled manner.

1.2 Ocular Drug Delivery Systems for the anterior region

Current ocular dosage forms span across liquids, semi-solids and solids which can be delivered via oral, topical, systemic or intraocular route [4]. An appropriate system is chosen depending on the pathophysiology of the condition, target region within the eye, the duration of treatment and patient profile. For conditions of the posterior eye region, intraocular injections are used to access the affected region irrespective of their invasive nature [12-14]. Oral administration is highly patient compliant but relies on the oral bioavailability of the drug. Systemic administration, although invasive, can ensure good bioavailability. However, the diffusion of orally and systemically administered drug is limited by the blood-retinal barrier in the posterior region and poses the potential for off-target drug-toxicities [12].

Currently, topical route is highly preferred for the management of anterior conditions of the eye such as dry eye syndrome, glaucoma, uveitis, allergic conjunctivitis and post-operative inflammation [15, 16]. Various drug delivery systems such as solutions, suspensions, gels, ointments, contact lenses and conjunctival inserts are used via the topical route [10].

1.2.1 Eye drops

Eye drops, such as solutions and suspensions, are still the most popular ocular drug delivery system for the anterior region. They account for almost 70% of marketed ophthalmic formulations due to their convenience, non-invasiveness, ease of administration and ease of manufacturing [10, 17]. Despite these advantages, the effective corneal bioavailability for most ophthalmic eye drop formulations is no more than 5% [5, 16] as most of the topically administered solutions are washed away after 15-30 seconds [4]. Interestingly, the rate of removal of instilled solution is directly

proportional to the volume instilled [10]. Therefore, just increasing the volume of administered dose might not be able to improve ocular bioavailability significantly. Other factors like variability in volume dispensed [18] and lack of dose uniformity in suspensions [19] may lead to improper dosing.

1.2.2 Ointments

Ointments are semi-solid, petrolatum-based dosage forms which are commonly used in drug delivery to the anterior region of the eye. Ointments are easy to administer but are ill-accepted due to their greasiness and vison-blurring and therefore, they are mostly used as night-time medications [10]. Self-administration of ointments by the patient may lead to variability in dosage due to variations in amount of ointment applied and may become runny over time causing loss in formulation and obstruction in vision. Effectively, there is a reduction in patient compliance.

1.3 Challenges in dose uniformity

Overall, the physiological barriers of the eye (Section 1.1), loss of instilled dose and low patient adherence are the major challenges in ocular drug delivery. In fact, patient adherence to long-term treatments have been found to be as low as 50% due to various reasons such as forgetfulness, side-effects, difficulty in administration, lack of immediate relief from symptoms and complex multi-drug regimens [20-22]. In one study [23], dose frequency was a major factor found to have a statistically significant association with non-compliance in ocular dosing regimens. Even patients requiring short-term treatments post glaucoma filtration surgery or cataract surgery, were

found to have low adherence to therapy as they are not familiar with the intensive frequency of topical treatment regimens [22]. This may lead to under-dosing and over-dosing resulting in irregular drug exposure and potential side effects. One way to reduce the dose frequency is to improve the ocular bioavailability, which in turn ensures better efficiency of the dose administered.

1.4 Strategies to improve ocular bioavailability in the eye

Some strategies to improve ocular bioavailability include using prodrugs [4], increasing drug solubility in formulation [10], enhancing drug penetration through cornea, colloidal formulations and improving the residence time of formulation [24].

Prodrugs approach is used to deliver pharmacologically inactive or less active derivative of the drug, which is more lipophilic. Latanoprost is an example wherein it is hydrolyzed by an esterase to its free carboxylic acid form, which is more potent [15]. The prodrug approach involves extensive studies to investigate both, the parent molecule and metabolite, and is a viable approach only for a few therapeutic moieties.

Poorly water-soluble drugs like cyclosporine, dexamethasone etc. have been solubilized using cyclodextrins and dendrimers, which form inclusion complexes and allow higher strength of dose [10, 25]. However, an appropriate choice of cyclodextrin is important to ensure release of drug from the complex when administered to the eye as it is only the free drug that can penetrate the lipophilic biological barriers [26].

Permeability enhancers such as surfactants, bile acids, chelating agents, and preservatives, have been used to increase ocular tissue penetration and bioavailability [4]. Since their mechanism

of action involves destabilization of the tear film, they also have the potential to damage the corneal epithelium and induce irritancy [25].

Colloidal systems such as micro/nano emulsions, microspheres, micro/nano particles, liposomes etc. allow for targeted and sustained drug delivery along with enhanced permeation [27]. *Ex-vivo* studies using a microemulsion of everolimus with pig cornea indicated therapeutic concentrations of the drug overcoming the challenges of solubility and stability [28]. Another study demonstrated a three-fold increase in *ex-vivo* ocular permeation of indomethacin drug by microemulsion approach as compared to conventional aqueous solution [29]. In general, microemulsion-based systems require critically designed surfactant/co-surfactant ratios to ensure stability of the formulation and also limited concentrations of the surfactants to prevent ocular irritation [17].

Polylactic-co-glycolide (PLGA), polycaprolactone and chitosan are some of the polymers used to develop micro/nano particulate systems. The drug may be attached, dissolved, encapsulated or entrapped in the polymeric matrix [30]. In one study [31], the delivery and AUC of a an anti-inflammatory peptide drug, vancomycin, was found to be sustained in the aqueous humor of rabbits by PLGA microspheres better than an aqueous solution of the drug. However, such particulate systems often demonstrate variable stability, low reproducibility and lower drug-entrapment capacities [10].

Therefore, there is a need for a stable, physiologically safe and patient-compliant method to improve ocular bioavailability of drugs. In view of the challenges of the systems discussed, another way to achieve that is by increasing the residence time of drug formulation within the ocular space.

1.5 Strategies to improve residence time of formulation

Various strategies have been considered to improve pre-corneal residence time of formulations such as in-situ gelling systems, mucoadhesive polymers and ocular inserts [32].

1.5.1 *In-situ* gelling systems

These systems undergo a viscosity increase when instilled in the eye as drops, thus increasing the pre-corneal retention and potentially slowing the drug elimination from the eye [10]. The changes in viscosity can be triggered by different stimuli such as pH, temperature or electrolyte composition. Poloxamer 407 and xylan are examples of temperature-sensitive hydrogels, carbomer is an example of pH-sensitive hydrogel whereas gellan gum and alginic acid are examples of ion-sensitive hydrogels used in *in-situ* gelling systems for ocular application [14].

A commonly studied temperature-sensitive polymer is poly (N-isopropylacrylamide) which forms a gel above 32 °C and lowers in its transparency. The stiff gel can sometimes get uncomfortable for the patient and the lowered transparency can interfere with vision [25]. Another thermosensitive triblock copolymer, PLGA-PEG-PLGA, demonstrated higher C_{max} and AUC of dexamethasone acetate than eye drops in rabbit eye.

Gelrite® is another polysaccharide that forms clear gels at low solid concentrations in the presence of mono and divalent cations in found in tear fluid. Timoptic-XE is a marketed formulation for the delivery of timolol maleate using this approach. Sometimes, the *in-situ* gelling systems also contain mucoadhesive polymers to enhance the pre-corneal residence further [25].

1.5.2 Mucoadhesive polymers

These are typically macro-molecular hydrocolloids with many hydrophilic functional groups. They adhere to ocular mucin via non-covalent bonds, thus ensuring prolonged contact of the formulation with the ocular tissue [10]. They can establish electrostatic, hydrophobic, Van der Waal's interactions and hydrogen bonding with mucus (Table 1).

Table 1: Theories pertaining to mucodhesion mechanisms
Adapted from [7, 33]

Theory	Description
Electronic theory	Adhesion is established due to the electrostatic attraction between negatively charged mucin and positively charged materials
Adsorption theory	Adhesive interactions are related to the establishment of hydrogen and Van der Waals bonding; hydrophobic effects and chemisorption may also contribute
Wetting theory	Adhesion is related to the ability of a mucoadhesive (when in liquid form) to spread over the mucus layer
Diffusion theory	Considers that adhesion is established by the interpenetration of macromolecular mucoadhesives with mucin fibers, as driven by a concentration gradient differential
Fracture theory	Relates adhesion with the force required for interfacial detachment of two previously joint solid surfaces
Mechanical theory	Adhesion is dependent on the roughness of two different surfaces and the available area for interaction

These interactions are, however, time dependent factors and would be greatly influenced by the shear forces in the biological system. If insufficient wetting occurs, the polymers would not untangle themselves to be able to interact with the mucus. Excessive exposure may lead to over

extension of mucosal bonds. Mucoadhesive polymers must also have sufficient flexibility and adequate surface free energies to allow wetting with the mucosal surface [34].

Table 2: Various mucoadhesive polymers used in drug delivery systems
Adapted from [35]

Type of polymer	Examples
Anionic polymers	Carbopol® Polycarbophil® Sodium alginate Sodium carboxymethylcellulose
Cationic polymers	Chitosan Thiomers
Nonionic polymers	Hydroxypropylmethylcellulose (HPMC) Hydroxypropylcellulose (HPC) Methylcellulose Polyethylene glycol Polyvinylpyrrolidone Hydroxyethylcellulose (HEC)

Hyaluronic acid (HA) is a natural macromolecule present in the eye and is proposed as a viscosity enhancing agent in many formulations. It has been successfully employed in tear substitutes in severe dry eye conditions. Its benefits are attributed to its viscoelasticity, similar biophysical characteristics as mucins and long-lasting hydration due to retention [36].

Poly (acrylic acid) and carbomers are some other mucoadhesive polymers which exhibit extensive hydrogen-bonding with mucins [36]. They provide tunable rheological properties to solutions at different concentrations which affects their interactions with the mucin on corneal epithelium. Their inherent anionic nature is similar to mucins; they have good lubricating properties

and hence, are also employed in artificial tear drops. However, concentration related blurring and discomfort are sometimes reported [37].

Cellulose based polymers are a class of cellulose derivatives commonly employed as viscosity enhancing agents in eye drops and components of soluble ocular inserts [36]. These will be discussed in detail in Section 2.0.

1.5.3 Ocular inserts

Ocular inserts are drug-impregnated devices used for long-term sustained delivery. They may be placed directly on the cornea or in the conjunctival region of the eye. These systems may insoluble, requiring removal after a certain time or may be designed to dissolve, erode or biodegrade in the ocular environment [25]. The ocular inserts discussed in this section are used for drug delivery to the anterior region of the eye.

Ocusert® (Alza Corporation, Palo Alto, CA) was one of the first commercial inserts approved to treat ocular hypertension. It consisted of a pilocarpine-alginate matrix sandwiched between ethylene-vinyl acetate to achieve a constant drug release over time. It was discontinued owing to unreliable control of intraocular pressure, leakage, difficulty in administration and irritation [25]. Since then, advancements were made in the field of ocular inserts designed to provide reliable, controlled and patient compliant delivery of drugs through biodegradable or dissolving inserts.

Surodex™ (Allergan Inc., Irwine, CA) implant is an example of biodegradable implant containing PLGA and HPMC enclosing dexamethasone. A single administration provided pain relief and anti-inflammatory effect to patients of cataract operation for up to 10 days [13].

Lacrisert® (Valenat Pharmaceuticals, Bridgewater, PA) is a soluble minirod of HPC indicated for patients with moderate to severe dry eye syndrome to provide relief up to 24 hours [38]. It measures 1.7 x 3.5 mm and is placed in the conjunctival region of the eye.

Dextenza™ (Ocular Therapeutix, Bedford, MA) is a recently FDA-approved bioresorbable ocular insert placed in the anterior region of the eye to deliver dexamethasone for management of post-operative inflammation [39]. The matrix contains 4-arm polyethylene glycol (PEG) N-hydroxysuccinimidyl glutarate as the primary bioresorbable polymer which can deliver the drug for up to 30 days. There are other commercial inserts such as Vitrasert® (Bausch and Lomb Inc., Rochester, NY) and Ozurdex® (Allergan Inc., Irwine, CA) which have been developed for prolonged drug delivery to the posterior region of the eye.

1.5.3.1 Contact lenses

Contact lenses have traditionally been used to correct visual acuity and for aesthetic purposes. However, they are increasingly being considered as a viable option for ocular drug delivery due to advancements in their manufacturing and potential to "personalize". Drug laden contact lenses are mainly categorized as either hydrogel-based (rigid) or silicone hydrogel-based (flexible) with the latter being more popular due to higher oxygen gas permeation allowing higher patient compliance [16, 40]. To achieve the desired rate of drug delivery, physical and chemical modifications of contact lenses are carried out such as molecular imprinting of drugs, soaking the lens with Vitamin E, incorporation of micro/nano particulate formulations within the lens matrix or sandwiching a polymeric film between two layers of lens [16]. Contact lenses have been used for pre and post-operative delivery of anti-inflammatory drugs such as dexamethasone [41] and vancomycin chlorhydrate [42], especially to achieve a sustained drug release for several hours after the surgery, which is a critical period for the patient.

Despite the advantages of contact lenses, they have a potential to affect the corneal physiology, transparency may be lost due to instability of incorporated formulation and the need for modifications to personalize the product for every patient [16].

1.5.3.2 Microneedles

Microneedles (MN) are arrays of micrometer (100 – 900 μm) sized needles initially developed for transdermal drug delivery due to painless, high efficiency and ease of drug administration [43]. Drug coated stainless-steel MNs, hollow glass MNs containing drug solution and polymeric dissolvable MNs have been used for intraocular delivery of various molecules such as drugs, proteins and DNA [4, 44, 45]. In one study [44], higher local drug concentrations and quicker therapeutic outcomes without repercussive inflammation was observed in the delivery of sodium fluorescein and pilocarpine to a rabbit animal model. Another study [46] demonstrated the use of methacrylated hyaluronic acid based self-implantable, dissolvable microneedle patches to deliver diclofenac and an anti-angiogenic monoclonal antibody to a corneal neovascularization mouse model. These patches, which were thumb pressed on the cornea, showed a 90% reduction in the neovascular area after 7 days of a single dose application.

Despite the advantages of MN delivery systems, low drug loading capacity and mechanical instability of needles are some of their most common challenges [47]. Additionally, they physically penetrate through biological membranes, which may not be patient compliant in cases where the ocular membranes are damaged or injured.

1.5.3.3 Polymeric films

Polymeric films are a type of ocular inserts wherein a single drug or a combination of drugs are dispersed in a polymeric matrix. Multiple studies with animal models have been carried out to establish the efficacy and safety of this platform [48]. An interesting study [49] evaluated the efficacy of gentamicin-loaded bioadhesive ophthalmic drug inserts (BODI®) versus a marketed eye drop, Tiacil®, in conjunctivitis dog model. The BODI®, in form of a polymeric film, contained mucoadhesive polymers such as HPC and Carbopol® 934. The clinical study reported similar recovery in both cases with the frequency of administration reduced significantly in case of insert.

A randomized, open-label clinical study compared the ocular bioavailability of sodium fluorescein from three eye drops and a lyophilisate [50] . It was demonstrated that the lyophilisate, which is similar a solid ocular insert, showed better bioavailability as opposed to the eye drop regimen for up to 7 hours. In another study [51] , the therapeutic efficacy in terms of intraocular pressure lowering effect of polyvinylpyrrolidone films was found to be sustained better than brimonidine tartarate solution until at least 8 hours. Therefore, polymeric films can sustain the delivery of drug moiety to achieve a prolonged therapeutic outcome with lowered frequency of administration.

The various advantages of using polymeric films are shown in Figure 2 [52].

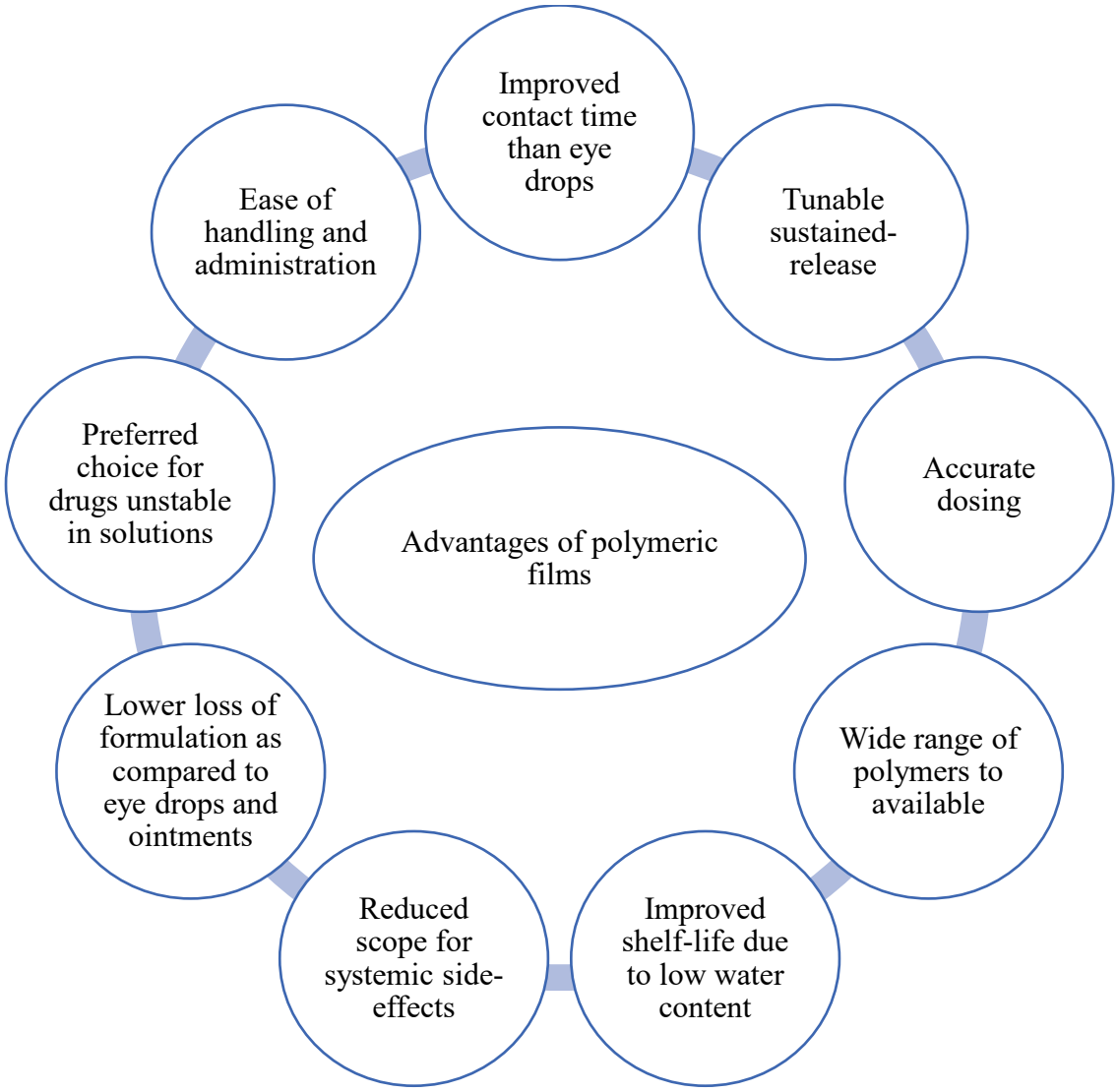

Figure 2: Advantages of using polymeric film as a drug delivery platform

1.6 Ocular inflammation and existing therapies

Anti-inflammatory agents have been widely used in management of dry eye, microbial infections, allergic conjunctivitis and post-operative management in the eye. The number of patients suffering from these conditions is on the rise due to pollution, changing climates, increased exposure to electronic screens and as a part of secondary complications associated with other

chronic diseases [53-55]. For management of these complications, anti-inflammatory agents in the form of eye drops and ointments are prescribed for various durations ranging from a few days to several months.

1.6.1 Allergic conjunctivitis

Allergic conjunctivitis is an ocular manifestation of exposure of an individual to allergens [56]. Ocular allergy affects 15-20% of the population in developed countries [15]. Some of the commonly used drugs to treat allergic conjunctivitis include olopatadine, ketotifen, ketorolac etc.[57]. Dosing regimens with eye drops can last for weeks with dose administration frequency ranging from 2-6 times per day [56]. These frequent administrations can increase the drug concentration significantly even though a symptomatic maintenance dose is required later in the day. With such intense dosing regimens, patient adherence is also challenged due to various reasons as discussed in Section 1.3, eventually affecting the outcomes of prescribed treatment.

1.6.2 Post-surgical ocular inflammation

Cataract surgery, surgery for management of glaucoma, vitreoretinal surgery and corneal transplantation are some of the most common surgical procedures performed by ophthalmic surgeons worldwide [58]. Corticosteroids and non-steroidal anti-inflammatory drugs in the form of eye drops are used to manage post-operative inflammation for a duration ranging from a few days to 3 months. For more serious cases of inflammation, corticosteroids such as difluprednate, prednisolone acetate and hydrocortisone are prescribed as opposed to antihistamine/mast-cell

stabilizers [59]. If the inflammation is not managed, chances of secondary ocular complications would increase [15].

1.6.3 Ocular inflammation due to microbial infection

Bacterial conjunctivitis is caused by pathogens such as staphylococci, streptococci, N gonorrhea etc. [60]. Ointments of tobramycin, gentamicin, erythromycin, bacitracin, polymixin B sulfate and prednisolone acetate are some of the FDA-approved products for ocular infection management [39]. However, some of these products inherently contain an anti-inflammatory drug, hydrocortisone, for the management of ocular inflammation and prevent further corneal destruction and scarring [61]. Similar to the antibiotic agents used, there is a need to ensure a sustained therapeutic outcome in terms of inflammation which can be achieved by controlling the release of the anti-inflammatory drug used. In addition to the discussed conditions, anti-inflammatory agents such as loteprednol and lifitegrast [62] are also used in the management of dry eye syndrome along with artificial tears.

Particularly for long-term treatments in management of ocular inflammation, there is a need to provide a platform for drug delivery that can reduce the burden of dosing on the patient and provide a simple, easy-to-administer, patient compliant drug delivery system. Polymeric films can be a viable option to deliver anti-inflammatory drugs due to their various advantages, as discussed in Section 1.5.3.3. However, considering the various physiological barriers of the eye, there is a need to ensure that the delivered dosage form is retained for a prolonged period. Taking inspiration from nature, a unique approach in the form of micropatterns has been proposed to potentially improve adhesion of polymeric films to ocular mucosa.

1.7 Microtopographic features to improve adhesion

The Gecko lizard is known for its ability to travel on vertical surfaces while defying gravity. Microscopic evaluations demonstrated that each Gecko foot has almost 500,000 keratinous projections known as setae. These setae are 30-130 μm long eventually terminating in sub-micron sized spatula-like structures [63]. Overall, the Gecko foot exhibited super hydrophobicity (contact angle of one seta > 160°) and high adhesive properties due to extensive Van der Waal's interactions between the setae and a surface [63, 64]. Gecko-inspired adhesives tapes have been developed and commercialized, such as Geckskin™ and nanoGriptech®.

Bioadhesives have also been developed using a biodegradable and biocompatible polymer, poly (glycerol-co-sebacate acrylate) wherein the nanotopography of the patterns were varied and studied for adhesion to porcine intestinal tissue (*in vitro*) and rat abdominal tissue (*in vivo*) [65]. The presence of nanopatterns of sizes between 0.1-1 μm showed nearly two-fold increase in adhesion forces. The authors envisioned development of this platform for wound-sealing application and a potential for simultaneous drug delivery. Topographical texturing using micropatterns has been patented by Boston Scientific (Maple Grove, MN) as a stent coating [66] and an mucus-plugging preventive device to be used within an airway [67] to ensure interlocking of implants at their intended biological sites. This highlights the extensive potential that topographical manipulations can have to improve the functionality of systems used for biological application.

Micropatterned surfaces were also studied for improvement in the frictional forces of endoscopic probes. Microcapsule endoscopes may miss their targeted area due to lack of control over position and orientation as it relies on gastrointestinal (GIT) peristalsis. Static friction force, which is indicative of the maximum force required to first move the sample on the tissue, was found

to be higher for patterned (140 μm) samples than unpatterned samples with a significant contribution from macroscale edge effects of the patterns [68].

Another study [69] demonstrated the effect of using micropatterned polydimethylsiloxane (PDMS) surfaces on rabbit intestinal tissue to correlate their functionality in self-propelled robotic systems in GIT. Larger micropatterns (>80 μm) showed greater friction coefficients as compared to non-patterned PDMS samples. In general, micropatterns on PDMS, in the range of 100 μm size were found to demonstrate higher friction forces. All these examples seem to be in accordance with the mechanical theory of mucoadhesion (Table 1).

Collectively, this suggests that micropatterns on polymeric substrates can enhance friction and interactions with a mucosal surface, which can be exploited to enhance residence time and avoid the limitations of conventional ocular drug delivery systems.

2.0 Rationale

Ocular inflammation is a common symptom of many eye diseases such as allergic conjunctivitis, microbial infections etc. and an undesirable consequence of ocular surgical procedures [70]. If left untreated, severe manifestations can arise, such as pain, discomfort, corneal edema and interference with rehabilitation of vision [71]. Corticosteroids are usually the first line of treatment for ocular inflammation management and due to their low-water solubility, they are primarily delivered in the form of ointments and suspensions [62]. Some other non-steroidal anti-inflammatory drugs such as olopatadine hydrochloride, ketorolac, chromolyn sodium etc. are also used in cases where management of intraocular pressure is critical or there is a risk of corneal melting and therefore, corticosteroids are avoided [62, 72]. The duration of treatment can vary from few days to several months [57, 58].

Challenges in treatment of ocular inflammation include high frequency of administration of anti-inflammatory agents, low patient adherence and variable drug exposure [20, 21]. Moreover, the existing dosage forms are limited by low patient compliance and losses of the administered dosage due to a variety of physiological challenges in the eye, as discussed in Section 1.1[22, 32]. The severity of these challenges is particularly critical when inflammation management is required in the anterior region of the eye for a prolonged duration for conditions discussed in Section 1.6 [56, 59]. To overcome these challenges, a delivery system is needed that can reside in the ocular space for prolonged period despite the physiological challenges of the eye and sustain the release of the drug. We are proposing a micropatterned film which can sustain the delivery of an anti-inflammatory drug to the anterior chamber for at least 72 hours by virtue of its chemical

composition (formulation) and improve the pre-corneal residence time through its physical characteristics (micropatterns).

Hydrocortisone (HCT) is a corticosteroid (Figure 3) [73] used for the management of inflammation resulting from microbial infections. Due to its poor water solubility (0.32 mg/mL at 25 °C) [73], it is commercially marketed as a suspension (1% w/v) or an ointment (1% w/w) with a recommended frequency of administration of every 3-4 hours. With such high dosing frequencies, patient compliance is challenged. Therefore, to provide a sustained delivery, we are proposing a polymeric film formulation due to the various advantages discussed in Section 1.5.3.3. Based on an average drop size of 30 µL, which corresponds to 300 µg of HCT per dose in commercial formulation, we intend to deliver 300 µg for up to 72 hours using a representative 13 x 13 mm micropatterned film.

Olopatadine hydrochloride (OLO) [74] has been one of the first-line treatment anti-inflammatory drugs used in the management of ocular inflammation associated with allergic conjunctivitis (Figure 4). Clinically, it is considered as a "gold-standard" in ocular inflammation management for its dual-action role as an antihistamine and a mast-cell stabilizer [62]. OLO is commercially available as a 0.2% solution (Pataday®, Alcon) and a 0.7% solution (Pazeo®, Alcon) which can provide relief for 18-24 hours [62]. The average administered dose is 200 µg per day for up to 6 weeks [75]. Owing to its high water solubility (> 20 mg/mL at 25 °C) [74], it is challenging to control its release in an aqueous tear-fluid environment. Therefore, to provide a sustained release of this hydrophilic drug, we are proposing a micropatterned polymeric film formulation aimed at delivering 600 µg of OLO over a period of 72 hours.

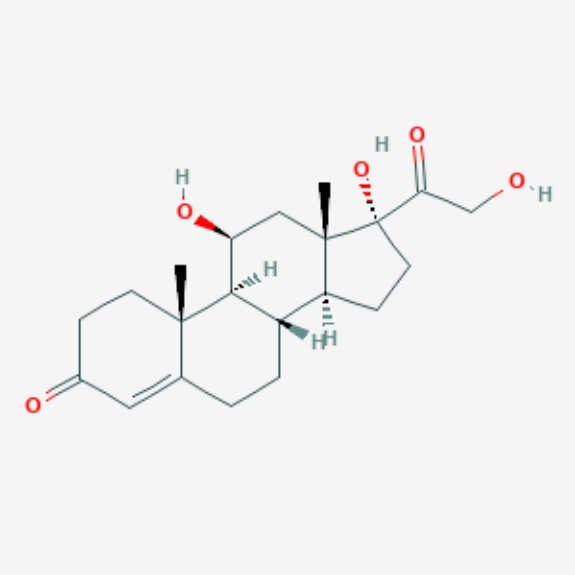

Figure 3: 2-D structure of hydrocortisone (HCT)

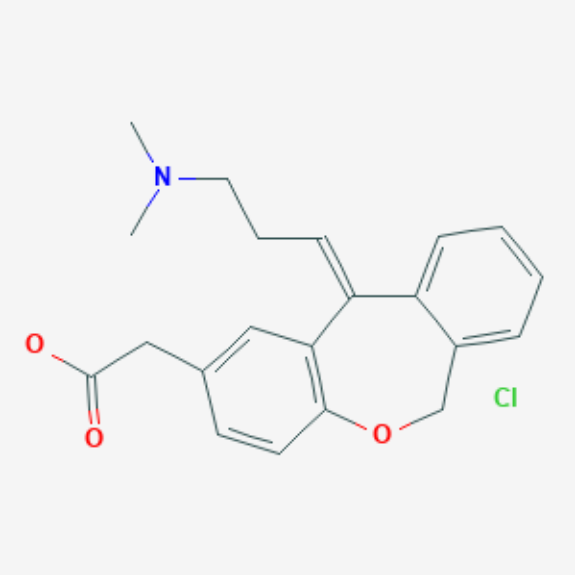

Figure 4: 2-D structure of olopatadine hydrochloride (OLO)

Various Generally Recognized as Safe (GRAS) - compliant polymers and plasticizers [76] were chosen as film excipients based on the suitability for ocular application and the requirement of sustained-drug delivery. The polymers could be broadly categorized into a water-insoluble polylactic-co-glycolic acid (PLGA) polymer and water-soluble cellulose-based polymers.

Considering the regulations by the FDA and corresponding guidelines provided by ICH Q3C (R7) [77] on residual organic solvents in drug products, formulations were restricted to aqueous or oil-in-water emulsion based film solutions.

HCT, being a hydrophobic drug, is expected to have greater interactions with a hydrophobic polymer. These interactions can be exploited to control the release of the drug for prolonged durations. A water-insoluble polymer, such as PLGA, would be expected to associate well with HCT and hence, control the drug release. PLGA is an FDA-approved, biocompatible and biodegradable polymer, extensively studied as a sustained delivery vehicle for drugs, proteins and other macromolecules [78]. In ocular drug delivery, it has been used in the form of micro/nanoparticles to deliver water-insoluble drugs like fluocinolone acetonide, dexamethasone etc. via intravitreal or subconjunctival injections [31, 36, 79]. PLGA has also been investigated for sustained release of water-soluble drugs such as vancomycin and calcitriol [31, 80, 81] due to its slow degradation in aqueous environment. In the proposed formulation, PLGA and HCT or OLO will be processed in an organic phase which will then be dispersed in an aqueous cellulose-based polymeric matrix. The cumulative effect of PLGA and the cellulose polymers could be tailored to obtain the desired release control of HCT or OLO up to 72 hours.

HPMC is a non-ionic, slightly mucoadhesive polymer used in various ocular formulations. It is used in eye drops for its good viscosity-enhancing and lubricant properties [36]. It is also used as a matrix component in oral tablets and film-forming polymer in mucoadhesive buccal films [82]. Various commercial grades of HPMC are available, which differ in the degrees of substitutions of methoxy and hydroxypropyl groups. These substitutions can affect the physicochemical properties of the polymer, such as, solubility and viscosity [83, 84]. These properties, in turn, can impact the interactions of polymers with drugs and allow for tunable controlled release of drugs [48, 83].

HPMC E5 is a low-viscosity grade with good film-forming properties [84]. On the other hand, HPMC K4M exhibits high viscosity when hydrated (Table 3), which can be exploited to control the release of drug from the system. Therefore, a combination of these two grades was used in the design of micropatterned films so that the drug release could be tuned by altering their ratios.

HPC is another non-ionic, inert polymer which has been found to improve the stability of tear film and hence used in dry eye syndrome management [85]. It is also known to have good film-forming properties and improves drug loading, stability and adhesion of films to other surfaces when blended with HPMC [84, 86]. Amongst the various grades of HPC, JXF grade is recommended for controlled drug delivery and has moderate molecular weight and viscosity (Table 3). Therefore, HPC JXF was chosen as another polymer for film formulation.

Hydroxyethyl cellulose (HEC) is also a non-ionic cellulose based polymer, and within the ocular environment, it is better tolerated than other cellulose polymers due to its low surface activity [36]. HEC 250L, a low-viscosity grade, was chosen since high viscosities was found to be challenging in the formation of micropatterns on films.

Table 3: Properties of cellulose-based polymers

Adapted from [87-89]

Polymer	Molecular Weight (Da)	Concentration (%w/w)	Viscosity (mPa sec^{-1})
HPMC E5	N/A	2	4-6
HPMC K4M	400,000	2	2700-5040
HEC 205 L	90,000	5	75-150
HPC JXF	140,000	5	150-400

Plasticizers can make films softer, smoother and reduce cracking which further improves the film toughness. These are particularly important when low-molecular weight polymers like HPMC E5 and HEC 250 L are used [84]. Also, since our formulation will be primarily aqueous-based, water-soluble plasticizers such as PEG 400 and propylene glycol were chosen.

The primary aim of choosing appropriate polymers of the film formulations was to sustain the delivery of HCT and OLO. The film can potentially be placed in the conjunctival region as it is the main site of macrophage invasion/inflammation response and provides a high surface area for drug permeation [11, 90]. However, due to the shear intensive processes in the eye such as blinking and eye ball movement [91], there is need to improve the residence time of the film in the eye. To address this, we propose incorporation of topographical features in the form of micropatterns, which can improve the adhesion of polymeric films (Section 1.7). The shape and dimensions of these micropatterns can influence the extent of adhesion [47, 92, 93]. Based on the previous work in our lab [93], micropatterns of circle, square and triangle shapes of 100 µm with an aspect ratio of 1:1, were chosen for our study. Therefore, films of 13 x 13 mm dimensions containing various compositions of discussed polymers and various shapes of 100 µm sized micropatterns were studied for the delivery of HCT and OLO.

3.0 Materials and Methods

3.1 Materials

Hydrocortisone USP (HCT) was obtained from PCCA (Houston, TX) and olopatadine hydrochloride (OLO) was purchased from Tokyo Chemical Industry (Tokyo, Japan). Polylactide-co-glycolide (Resomer® RG 502H) was graciously gifted by Evonik Industries (Piscataway, NJ). Hydroxypropyl methylcellulose (HPMC) K4M (Methocel™ K4M, Colorcon), HPMC E5 (Methocel™ E5 Premium LV, Dow Chemical Co.), hydroxypropyl cellulose (HPC) (Klucel™ JXF, Ashland), hydroxyethyl cellulose (HEC) 250 L (Natrosol ™ 250 L Pharm, Ashland) were the various polymers used in formulations. Other excipients, such as, polyethylene glycol (PEG) 400 and propylene glycol were purchased from Spectrum Chemical (Gardena, CA). Dichloromethane was obtained from Sigma-Aldrich (St. Louis, MO), Ethanol was purchased from Decon Laboratories (King of Prussia, PA) and ultrapure water was obtained from in-house Milli-Q® Direct 8 water purification system. For soft-lithography, Sylgard™ 184 Silicone Elastomer Kit was procured from Dow Corning Corporation (Midland, MI).

3.2 Methods

3.2.1 Fabrication of PDMS molds

Standard photolithographic and soft-lithographic techniques were used to make the PDMS molds [94, 95]. Briefly, Autodesk AutoCAD software 2018 was used to design photomasks containing concentrated regions of different shapes of 100 μm sizes (Table 4). These photomasks were used to develop SU-8 master templates. A silicon substrate of 8" diameter was spin-coated with SU-8 photoresist. The photomask with patterns was placed over this and the assembly was exposed to ultraviolet (UV) light to allow crosslinking of the exposed regions (patterns). This was followed by washing off the non-crosslinked SU-8 photoresist, as per the manufacturer's recommendations. Hence, the patterned SU-8 master template was developed using a photolithographic technique. PDMS was then cast on this template using a 10:1 ratio of Silicone Elastomer Base and Silicone Elastomer Curing Agent. The PDMS mold, which serves as a "negative template", was delaminated and used for subsequent film casting [96].

Table 4: Size and alignment of various micropatterns

Shape	Size of pattern (μm)	Distance between adjacent patterns (μm)	Nomenclature
Circle	100	100	100C100
Square	100	100	100S100
Triangle	100	100	100T100

3.2.2 Fabrication of micropatterned film

Films were fabricated using a solvent-cast method. Polymer dispersion in water was poured on a PDMS mold and subjected to vacuum cycles for 30 mins to remove entrapped air bubbles. It was then allowed to rest at room temperature for 1 hour and dried in the oven at 65-70°C and atmospheric pressure for 13-15 hours to form the micropatterned film. The film was peeled off from the PDMS mold and stored in aluminum foil. A schematic of the design and fabrication of micropatterned films is shown in Figure 5.

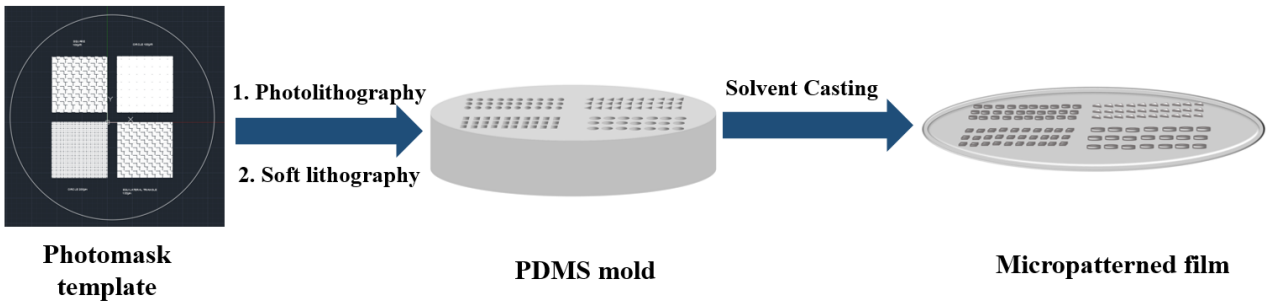

Figure 5: Design and fabrication of micropatterned films
Photomask template design is used for photolithographic and soft-lithographic techniques to develop PDMS mold which is in turn used to cast polymeric films

3.2.3 Film formulations

The various components of film formulations were adapted as per the discussion in Section 3.2.3. The formulations were broadly categorized into two types: Cellulose-based (Table 5) and Cellulose with PLGA (Table 6). To determine the effect of high-viscosity polymer on the drug release, two concentrations of HPMC K4M, 1.5% w/w and 0.75% w/w, were chosen. These formulations are referred to as, **1.5% K4M** and **0.75% K4M**, respectively. Additionally, two compositions with relatively higher HEC 250L, 4% w/w and 9% w/w, were also investigated. These will be referred to as **4% 250L and 9% 250L**. The solid content was maintained at 7.5% w/w for all cellulose-based formulations, except **9% 250L**.

The PLGA-containing films followed similar nomenclature as cellulose-based films, except for the additional term "PLGA" at the end (Table 6). The solid content in PLGA-based films was maintained at 9.375 %w/w.

Table 5: Compositions of cellulose-based films

Component	1.5% K4M (%w/w)	0.75% K4M (%w/w)	4% 250L (%w/w)	9% 250L (%w/w)
HPMC K4M	1.5	0.75	0	0
HPMC E5	1.5	2.25	1.5	1.25
HEC 250L	1.5	2.25	4	9
HPC JXF	3	3	2	1
PEG 400	1.125	1.125	1.125	1.6875
Propylene Glycol	0.75	0.75	0.75	1.125
Water	90.625	90.625	90.625	88.9375

Table 6: Compositions of cellulose and PLGA - based film formulations

Component	1.5% K4M PLGA (%w/w)	0.75% K4M PLGA (%w/w)	4% 250L PLGA (%w/w)
PLGA 502H	1.875	1.875	1.875
HPMC K4M	1.5	0.75	0
HPMC E5	1.5	2.25	1.5
HEC 250L	1.5	2.25	4
HPC JXF	3	3	2
PEG 400	1.125	1.125	1.125
Propylene Glycol	0.75	0.75	0.75
Dichloromethane	6.5625	6.5625	6.5625
Water	82.1875	82.1875	82.1875

As PLGA is water-insoluble [78], DCM was used to dissolve the PLGA which was then dispersed in the aqueous phase. The PLGA content in films was limited as per the formulations listed in Table 6 since the amount of DCM in the system would have to be restricted. PDMS has a tendency to swell and dissolve in organic solvents like DCM [97] and hence, would be challenging for film solutions made with high organic solvent content. A swollen PDMS mold would have altered micropattern dimensions and therefore, inaccurate micropatterns on films. In our formulations, the DCM phase was found to be uniformly dispersed like an emulsion in the viscous cellulose-polymer matrix. No phase separation was observed until the solutions were poured into the PDMS molds or even in the dried films suggesting that we can incorporate hydrophobic polymers in the micropatterned film platform by dispersing them in an aqueous matrix.

3.2.4 Preparation of drug-loaded polymer dispersions

To make a film using one PDMS mold, 21.3 g of cellulose polymer dispersion was prepared using the appropriate formula, as listed in Table 5 and Table 6. Plasticizers and cellulose polymers were added to water and subjected to 10 minutes of sonication.

For cellulose-based OLO films, 28.8 mg of drug was directly added to this solution whereas for HCT films, 14.4 mg of drug was dissolved in 0.6 mL DCM and added dropwise to the solution. For PLGA containing films, the drug and PLGA were dissolved in 1.4 mL DCM. The DCM solution was added dropwise to the aqueous phase. These mixtures were allowed to stir overnight to get a uniform emulsion. This was later cast using the procedure described in Section 3.2.2.

3.2.5 Physical characterization of films

At least three samples for every film were characterized for their weight, thickness and tensile properties.

3.2.5.1 Weight and thickness

Micropatterned films were weighed using an analytical balance (Mettler Toledo, XS105 DualRange and Mettler Toledo, AB104-S/FACT). The film thickness was measured in 3 regions spaced out randomly, using a thickness gauge (Mitutoyo, Absolute) for each of the various shapes of 100 μm patterns.

3.2.5.2 Tensile properties

Tensile strength of films was measured using a texture analyzer (TA.XT *Plus* C, Stable Microsystems), tensile grips and associated software (Stable Microsystems, Exponent). The test parameters used were as follows:

Test mode: Tension; Test Speed: 3 mm/sec; Target Mode: Distance; Distance: 140 mm

A film sample of known dimensions (approximately 1 inch x 0.5 inch) was held between the tensile grips. The grips pulled the film sample at a constant rate and the maximum force required to break the film was used to calculate the tensile strength of the film using the following formula:

Tensile strength = Maximum force (kg)/Area of films (m^2)

3.2.6 Drug content

Simulated Tear Fluid (STF) was prepared as per the composition shown in Table 7. Since it was the media of choice for dissolution testing of films, standard curves of HCT and OLO were plotted for solutions in STF.

3.2.6.1 HCT standard curve

Standard curve of HCT was plotted in the range 2-25 µg/mL in STF at 248 nm, which was the wavelength of maximum absorption. To determine the drug content of films, a standard curve was also plotted in the range of 2-25 µg/mL in 50% ethanol in Milli-Q water at 245 nm. HCT-loaded film samples (13 x 13 mm) were dissolved in 15 mL of 50% ethanol using sonication. The solutions were then vortexed, centrifuged at 300 g for 20 minutes and the supernatant was analyzed using UV (NanoDrop One^C, Thermo Scientific) at 245 nm. These assay samples were found to be stable for 48 hours, when stored at room temperature (25-30 °C) protected from light.

3.2.6.2 OLO standard curve

Standard curves of OLO were plotted for the range of 10-150 µg/mL at 299 nm in STF and Milli-Q water. Drug content of films was determined by dissolving 13 mm x 13 mm samples in 5 mL of Milli-Q water followed by centrifugation and analyzed using UV at 299 nm.

Table 7: Simulated Tear Fluid (STF) composition
Adapted from [98]

Component	%w/v in water
Sodium bicarbonate	0.2
Calcium chloride dihydrate	0.008
Sodium chloride	0.67
10% Hydrochloric acid	Used to adjust pH to 7.4

3.2.7 Drug release study

To determine the kinetics of drug release of various formulations, an *in vitro* release study was carried out.

3.2.7.1 HCT release from micropatterned films

HCT film samples of 13 mm x 13 mm dimensions containing 300 µg drug were weighed and used for the release study. Sink conditions were maintained using 10 mL STF in 15 mL centrifuge tubes. This assembly was kept at 37 °C and 100 revolutions per minute in a shaker-incubator. Samples of 2 mL were withdrawn from the tubes at pre-determined intervals (30 mins, 1 hour, 2, 4, 6, 8, 10, 12, 24, 48, 72 hours) and replenished with equivalent fresh media every time.

Each collected sample was centrifuged at 14000 rpm for 10 minutes and the supernatant analyzed using UV spectrophotometry at 248 nm.

3.2.7.2 OLO release from micropatterned films

OLO film samples of 13 mm x 13 mm, with a target 600 µg drug content, were weighed and studied for drug release. Considering the drug loading and solubility of OLO, sink conditions were maintained using 5 mL STF in 15 mL centrifuge tubes. The assembly was maintained at 37 °C and 100 revolutions per minute in a shaker-incubator. Samples of 1 mL were withdrawn at pre-determined intervals (30 mins, 1 hour, 2, 4, 6, 8, 10, 12, 24, 48, 72 hours) and replenished with equivalent fresh media. Each collected sample was centrifuged at 14000 rpm for 10 minutes and the supernatant was analyzed using UV spectrophotometry at 299 nm.

3.2.8 Differential Scanning Calorimetry

Differential Scanning Calorimetry (DSC) was performed using Mettler Toledo to study the interactions of drugs with polymeric excipients. Pure drug samples and physical mixtures with individual polymers or polymeric blends were subjected to DSC analysis. Considering the drug-loading in the formulations (Section 3.2.4) and the sensitivity of the instrument, all physical mixture samples were prepared in a 1:1 ratio of drug to polymer(s). Thermograms were obtained by heating HCT samples from 25 °C to 240 °C at a rate of 10°C/min. OLO samples were heated from 25 °C to 300 °C at a rate of 10°C/min. Nitrogen gas was purged through the system at 50 mL/min during all sample runs.

3.2.9 *Ex-vivo* tissue mucoadhesion

Some experimental reports state that the frictional forces involved in removal of Gecko foot from surface are higher than the adhesive forces involved in adhering to the surface. These adhesion forces in turn depend on the shear forces (friction and gripping) and the gripping direction [99]. Since the eye also involves various shear forces which may challenge the adhesive strength of the film, we have used frictional forces as a measure of mucoadhesive strength of the films rather than conventional methods, which only consider forces in axial direction [33, 35, 100].

The mucoadhesive performance of micropatterned films with unpatterned control was tested using a method developed in-house, inspired from methods used for frictional evaluation in other studies [68, 69]. The ex vivo mucoadhesion testing of films was carried out using a texture analyzer (TA.XT *Plus* C, Stable Microsystems), a 5-kg load cell and a controllable sliding platform (XSlide™, Velmex Inc.). The film sample was attached to the head of a cylinder probe of 8 mm diameter (TA-24) using double-sided adhesive tape. Porcine intestinal tissue stored at -80 °C was thawed to room temperature and then washed with simulated tear fluid. Keeping the ocular system in perspective [7], excess mucus was removed using blotting paper. The tissue, with the mucosal side facing upwards, was secured between a compression probe (CPC 20-T, ADMET) and a 0.125" thick 316 stainless steel round shim with clamps. This assembly was placed on the sliding platform below the cylindrical probe. The entire assembly is as shown in Figure 6.

Compressive pre-loading with a force of 10g for a period of 30 seconds was performed by bringing the micropatterns in contact with the porcine tissue. The loading force was chosen on the basis of the values reported in literature [101] in order to capitulate ocular shear forces and also based on the sensitivity of the load cell used.

With micropatterns in contact with the tissue, the tissue was moved in horizontal direction at a rate of 0.05 cm/sec for 5 secs to cover a distance of 0.25 cm. The Exponent software reported the changes in forces experienced by the probe in response to the shear created by the sliding tissue. The work expended in this process is a result of frictional barriers and was quantified in the form of area under the curve. These values were used as an indirect indication of the mucoadhesive potential of films being tested.

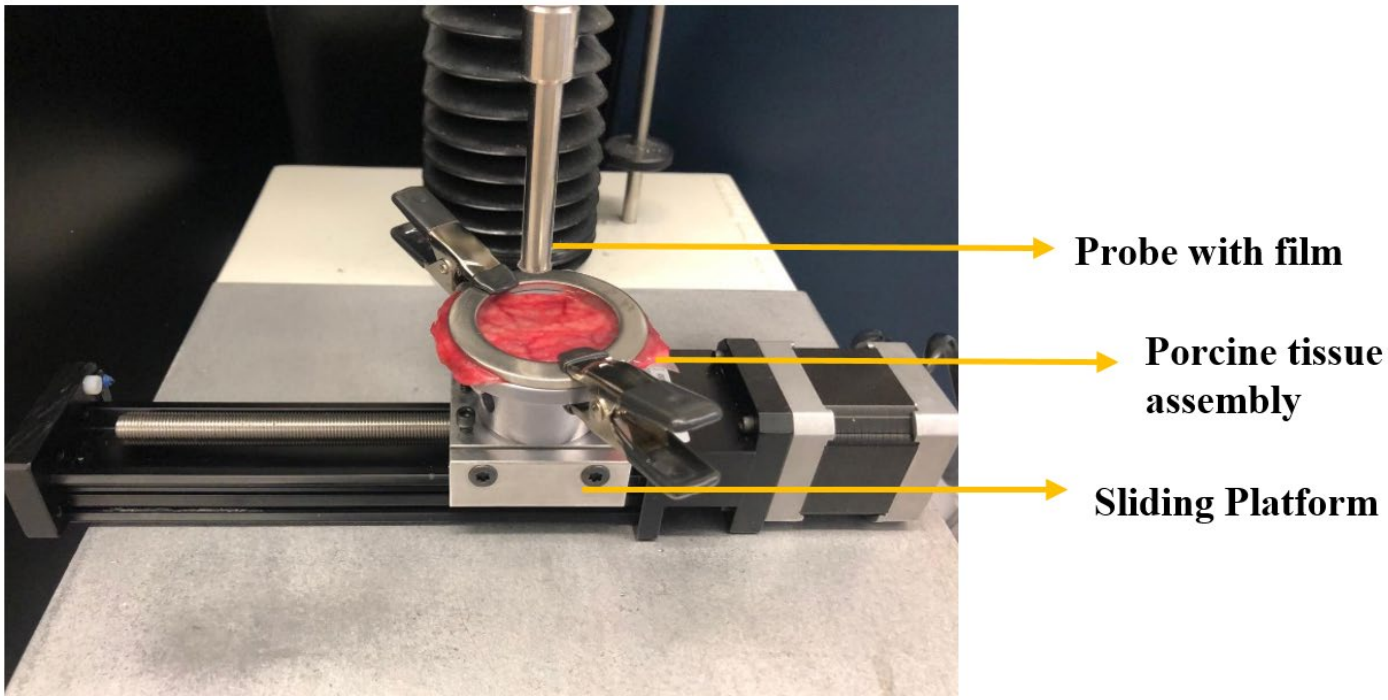

Figure 6: *Ex vivo* mucoadhesion assembly
Probe with micropatterned film made to contact porcine tissue with 10g force for 30secs followed by horizontal movement of the tissue against the frictional force of film for 0.25 cm at the rate of 0.05 cm sec^{-1}

4.0 Results and Discussion

4.1 Fabrication of micropatterned films

FITC-loaded films were visualized using confocal microscopy to confirm the formation of three dimensional micropatterns. The patterns were uniformly developed and filled for all 100 µm shapes, as seen from the vertical and horizontal panels of Z-stacking in Figure 7. Therefore, we successfully manufactured films with 100 µm-sized patterns using soft-lithography for the formulations listed in Table 5 and Table 6.

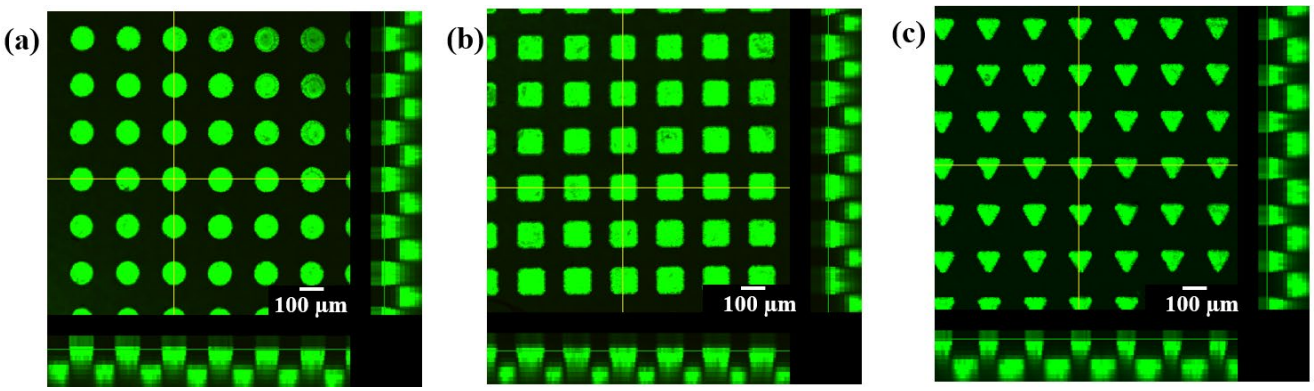

Figure 7: Formation of micropatterned films
Confocal images of FITC-loaded films with horizontal and vertical panels indicating the signal intensity as a result of Z-stacking across the thickness of films for (a) 100C100; (b) 100S100; (c) 100T100

To visualize the distribution of hydrophobic PLGA and other water-soluble polymers within the film, FITC and Nile Red were added to the aqueous and organic phase, respectively. FITC would be associated with the cellulose polymers and Nile Red would be associated with the PLGA. The confocal images of micropatterned film showed uniform distribution of red fluorescence

suggesting that PLGA is uniformly dispersed in the cellulose polymer matrix. (Figure 8). Differential interference contrast (DIC) microscopy also corroborated with these observations. DIC images of cellulose films and PLGA containing films are shown in Figure 9. A uniform polymeric matrix can be seen in both cases indicating that the PLGA has been uniformly dispersed.

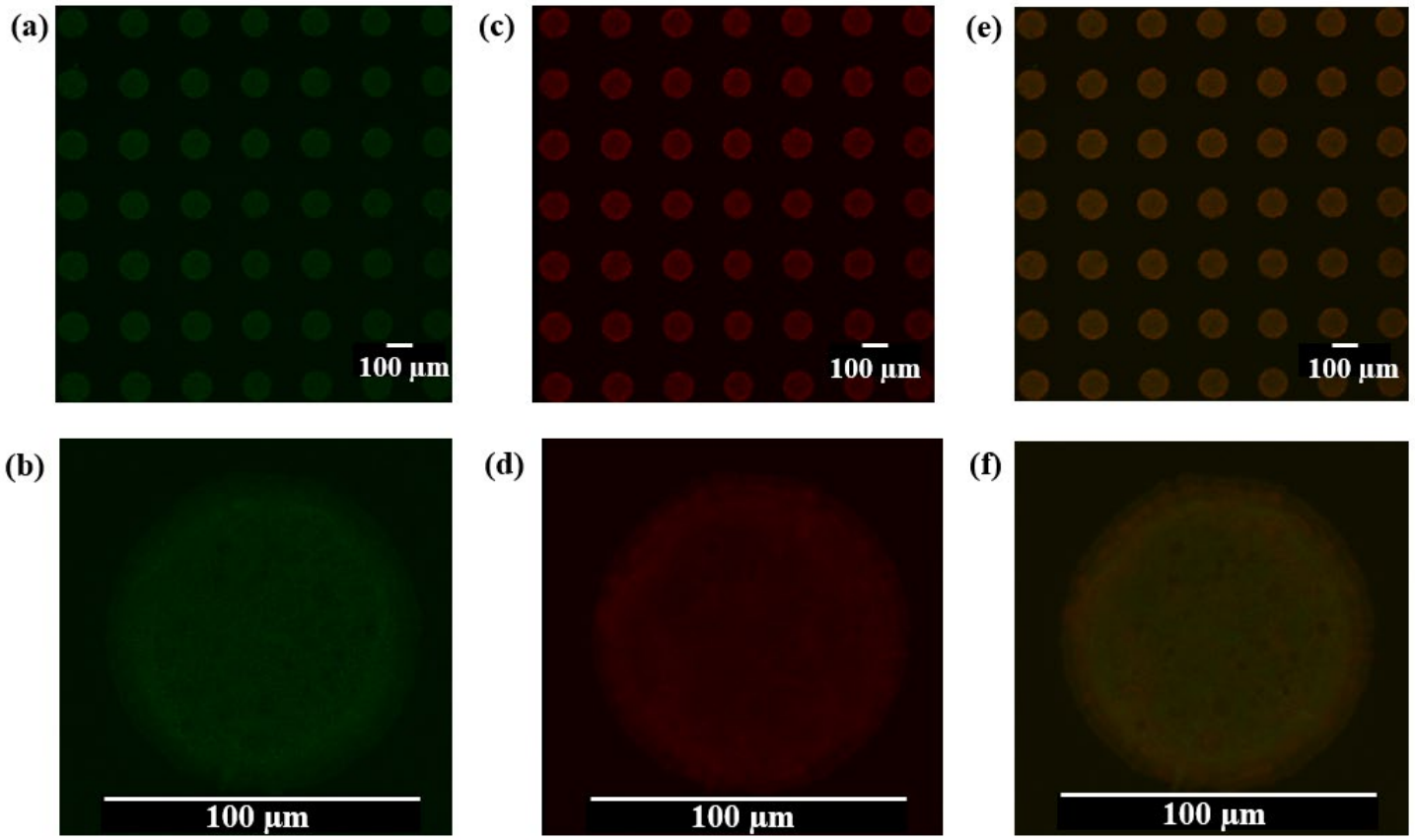

Figure 8: Spatial distribution of aqueous and organic phases
Confocal images of 100C100 micropatterned films (a) Green color of FITC (aqueous dye) showed uniform distribution of cellulose polymers, (b) Red color of Nile Red (organic dye) showed uniform distribution of PLGA, (c) Merge channel indicated uniform distribution of both phases, (b)-(f) Higher magnification images of the conditions in (a)-(c)

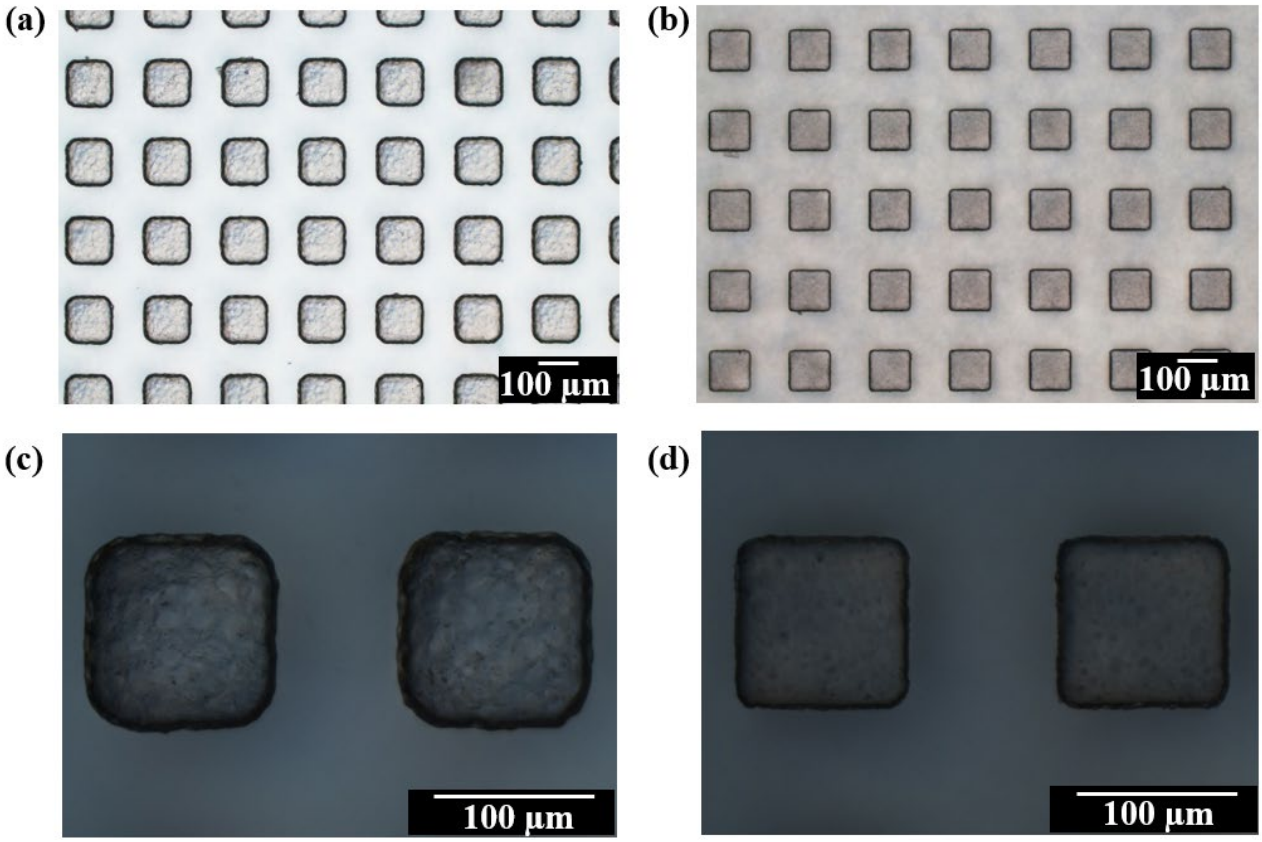

Figure 9: Uniform distribution of PLGA and cellulose matrix
DIC microscopy images of 100S100 micropatterned films. Comparison of (a) 4% 250L and (b) 4% 250 PLGA showed no phase separation of PLGA polymer indicating that PLGA is uniformly distributed in the cellulose polymer matrix in PLGA containing films, (c) - (d) Higher magnification images of (a) – (b)

4.2 Film characterization

All micropatterned were characterized for their weight, thickness and drug content, as shown in Table 8 and Table 9. For both HCT and OLO films, the drug content was found to be uniform over the different micropatterns within the same film.

Table 8: Phyical characteristics of HCT micropatterned films

*Weight and drug content of entire film is reported, #Thickness is average of circle, square and triangle micropatterned film, Data is reported as Mean ± S.D (N=3)

Film	Weight* (g)	Thickness# (mm)	Drug content* (mg)
1.5% K4M	1.981 ± 0.027	0.294 ± 0.005	13.765 ± 1.776
0.75% K4M	1.988 ± 0.026	0.236 ± 0.005	14.918 ± 1.6
4% 250L	1.906 ± 0.05	0.263 ± 0.008	14.241 ± 1.582
1.5% K4M PLGA	2.137 ± 0.021	0.253 ± 0.01	15.608 ± 3.37
0.75% K4M PLGA	2.167 ± 0.011	0.245 ± 0.008	12.828 ± 1.666
4% 250L PLGA	2.283 ± 0.022	0.25 ± 0.032	15.043 ± 2.05

Table 9: Phyical characteristics of OLO micropatterned films

*Weight and drug content of entire film is reported, #Thickness is average of circle, square and triangle micropatterned film, Data is reported as Mean ± S.D (N=3)

Film	Weight* (g)	Thickness# (mm)	Drug content*(mg)
1.5% K4M	2.095 ± 0.006	0.24 ± 0.008	27.312 ± 1.867
0.75% K4M	2.027 ± 0.053	0.241 ± 0.021	27.963 ± 1.686
4% 250L	1.897 ± 0.031	0.276 ± 0.008	29.235 ± 4.426
9% 250L	2.932 ± 0.014	0.32 ± 0.008	29.092 ± 0.779
1.5% K4M PLGA	2.643 ± 0.194	0.255 ± 0.005	26.485 ± 5.46

4.3 Comparison of shapes for surface area and volume

The different shapes of micropatterns can vary in the surface area and volume. These variations can potentially impact properties of the films such as drug release and mucoadhesion [102]. The drug release and mucoadhesion of films are dependent on interfacial properties of polymers used in the formulation, surrounding media and the mucus and hence, the surface area could play a significant role in altering them. Table 10 lists the theoretical calculated parameters for various shapes of 100 µm size.

Table 10: Comparison of theoretical surface area for various patterns for a 13 mm x 13 mm film

Shape	Size (µm)	Number of patterns	Additional area of patterns (mm^2)	Additional volume of patterns (mm^3)	Total surface area (mm^2)	Total volume (mm^3)
Circle	100	4225	132.665	3.318	470.665	28.668
Square	100	4225	169	4.225	507	29.575
Triangle	100	4225	126.75	1.829	464.75	27.179

4.4 Release of HCT from micropatterned films

4.4.1 Effect of micropattern shape on HCT release

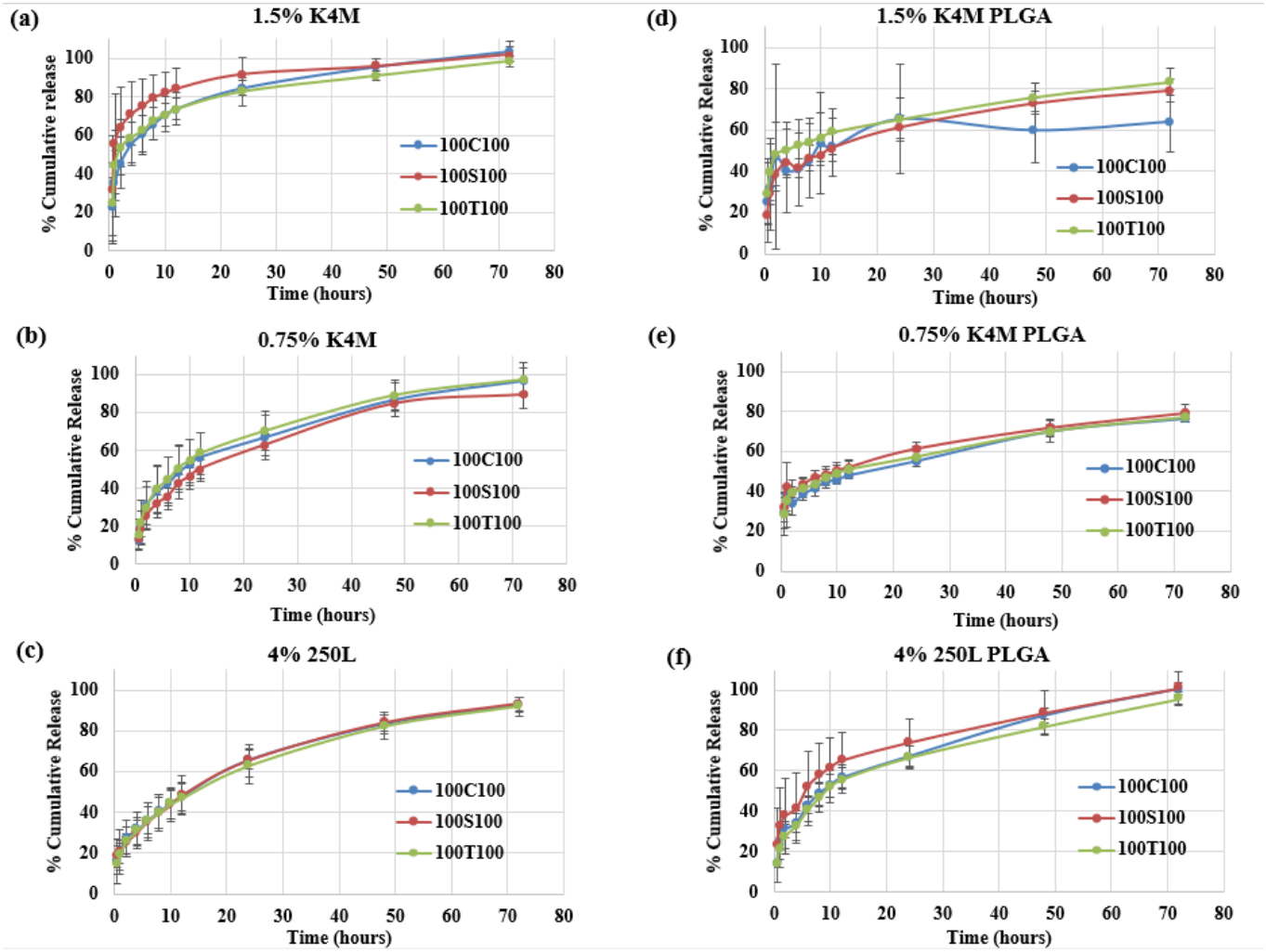

Figure 10: Effect of shape on *in vitro* release of HCT
Cumulative release of HCT from (a) 1.5% K4M, (b) 0.75% K4M, (c) 4% 250L, (d) 1.5% K4M PLGA, (e) 0.75% K4M PLGA, (f) 4% 250L micropatterned films evaluated using simulated tear fluid as release media. Data shown is the mean ± standard deviation for three replicates (n=3)

The release profile of HCT, from films containing circle, square and triangle shaped micropatterns of 100 µm size, are shown in Figure 10. Analysis using Repeated Measures (RM) two-way ANOVA test [103] indicated no significant effect of shape on the release profiles of HCT from various film compositions. Therefore, the drug release data for different shapes was combined for comparison of formulations in subsequent sections.

4.4.2 Effect of film composition on HCT release

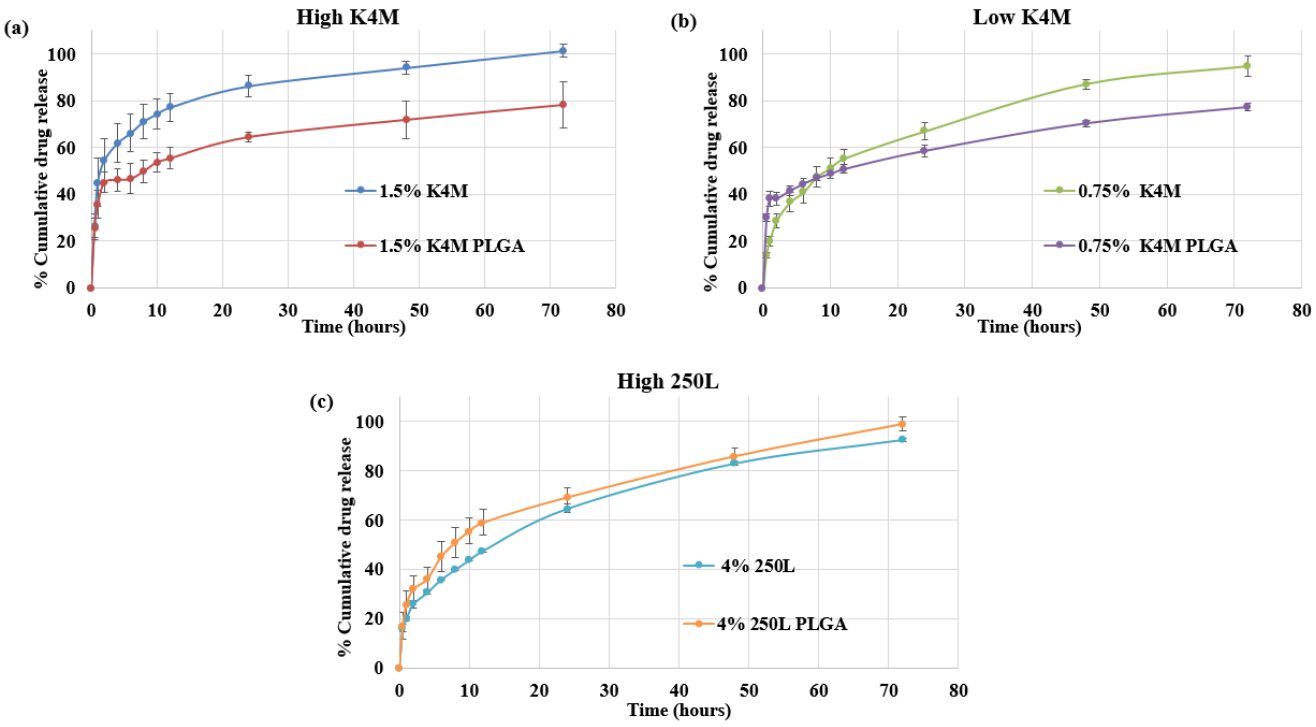

Figure 11: Effect of PLGA on *in vitro* release of HCT
Cumulative HCT drug release from (a) 1.5% K4M, (b) 0.75% K4M, (c) 4% 250L series (cellulose-based and PLGA-containing) micropatterned films in simulated tear fluid as release media. Data shown is mean ± standard deviation of three micropattern shapes from each of the three replicates (n=9)

The release profile of HCT from films of various compositions is shown in Figure 11. An initial burst release of at least 45% was observed within 2 hours for the films, 1.5% K4M and 1.5% K4M PLGA (High K4M). Beyond this time, the PLGA containing film showed sustained release of HCT as compared to its cellulose-based counterpart until 72 hours. For the low K4M content films, 0.75% K4M and 0.75% K4M PLGA, the initial burst release profiles were significantly different; the PLGA containing film released almost 40% within 2 hours whereas the cellulose-based film released 30% of the drug. This difference was present until 8 hours, after which the 0.75% K4M PLGA sustained the HCT release better than 0.75% K4M until at least 72 hours. In films with high HEC content, 4% 250L and 4% 250L PLGA, the initial burst release and subsequent release up to 72 hours was similar for both films.

In general, PLGA was found to sustain the release of HCT better than the cellulose films after initial burst release. This may be attributed to the association of HCT with PLGA, both being hydrophobic moieties, allowing the drug to get released slowly. To study the effect of K4M (high viscosity polymer) concentration, the release of HCT from 1.5% K4M and 0.75% K4M were compared. Surprisingly, 1.5% K4M (high conc.) film showed faster drug release than 0.75% K4M (low conc.) and 4% 250L (No K4M). However, the lowered K4M concentrations were compensated with HPMC E5 and HEC 250L, which may be imparting some other effects.

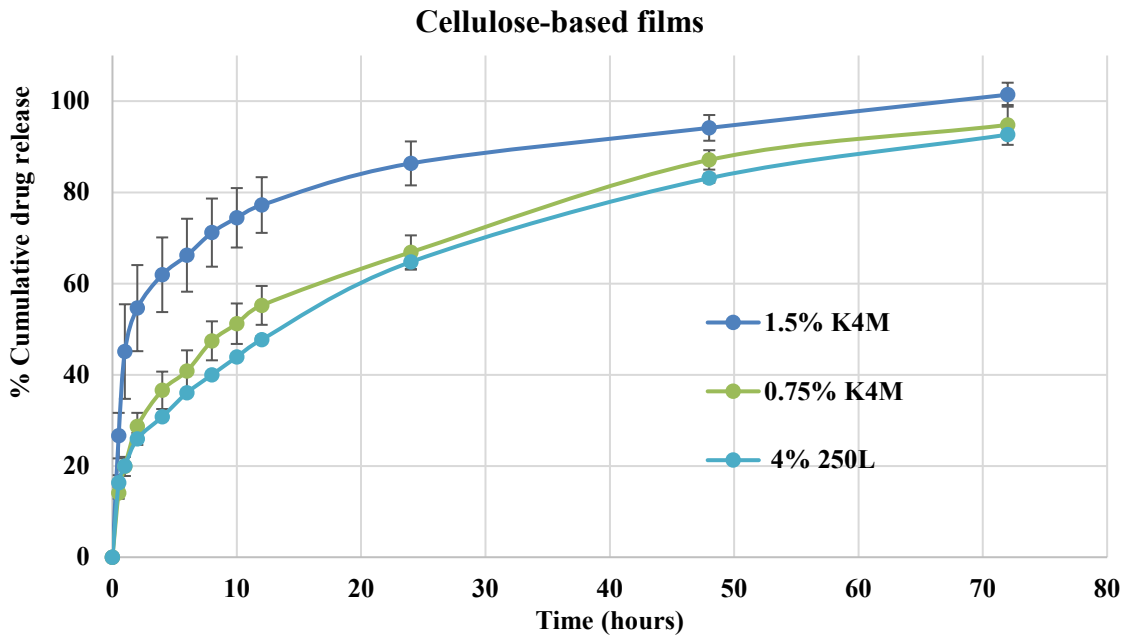

Figure 12: Effect of formulation on *in vitro* release of OLO
Cumulative release of OLO from various cellulose-based formulations, 1.5% K4M (high K4M), 0.75% (low K4M) and 4% 250L (high 250L) content in simulated tear fluid as release media. Data shown is mean ± standard deviation of three micropattern shapes from each of the three replicates (n=9)

Overall, drug release was sustained better with higher HEC 250L concentrations until 48 hours (Figure 12). Alternatively, PLGA could also sustain the drug release better than pure cellulose formulations with K4M. To investigate this further, the interactions of HCT with the various polymers were studied using DSC analysis.

4.4.3 Study of HCT- polymer interaction by DSC

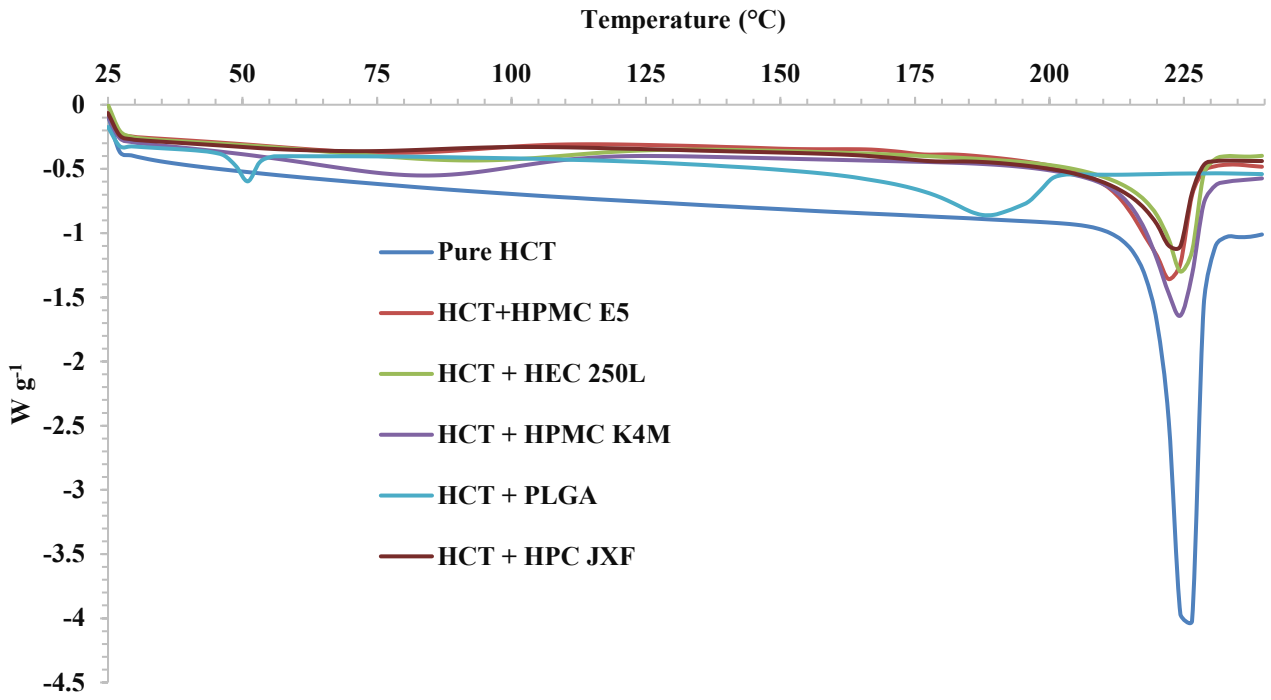

Figure 13: DSC thermograms of HCT and 1:1 physical mixtures of HCT with individual polymers
DSC analysis was carried out by heating samples from 25 – 240 °C at the rate of 10 °C/min. Heat flow data expressed is per gram of sample.

DSC analysis of HCT and its mixtures with polymers is shown in Figure 13. Pure HCT exhibited a sharp endothermic peak indicative of meting point at 224 °C with an onset at 220 °C. Pure PLGA also exhibited an endothermic event between 50-55 °C, typical of a glass transition peak. The cellulose polymers indicated no such behavior in this temperature range.

The 1:1 physical mixtures of HCT with individual cellulose polymers (HPMC E5, HPMC K4M, HEC 250L and HPC JXF) exhibited no significant shifts in the melting endotherm of HCT unlike the physical mixture with PLGA, where a substantial shift was observed to 188 °C (Figure 13). A shift in the endothermic peak of a drug is indicative of drug-polymer interactions [104, 105]. Therefore, it can be hypothesized that HCT interacts significantly with PLGA as compared to other

cellulose polymers. The different cellulose polymers affected the intensity and area under the peaks, which are representative of the enthalpy changes in the system [106]. Since all thermograms have been normalized to drug-polymer ratio and weight of the sample, the variations in area under the peak for different polymers may be indicative of differences in weak interactions of polymers with the drug.

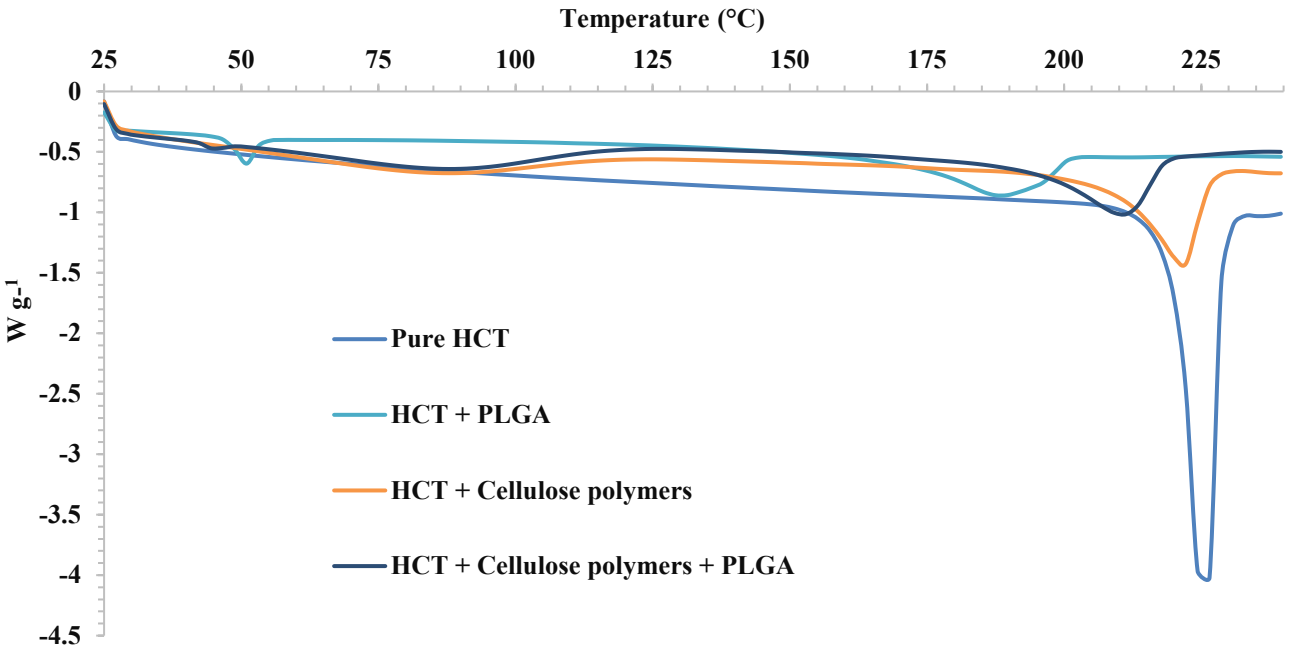

Figure 14: DSC thermograms of HCT and 1:1 physical mixtures of HCT with polymeric blends
DSC analysis was carried out by heating samples from 25 – 240 °C at the rate of 10 °C/min. Heat flow data expressed is per gram of sample.

To check the cumulative effect of polymeric blends on HCT, thermograms were also plotted for its 1:1 mixtures with the 1.5% K4M and 1.5% K4M PLGA polymeric blends, representative of the cellulose-based and PLGA containing formulations, respectively (Figure 14). The PLGA-containing formulation exhibited a greater shift (211 °C) than the cellulose blend (223 °C), validating the initial observation of PLGA interaction with HCT. Greater shifts with PLGA may be

due to the hydrophobic nature of both HCT and PLGA, allowing more interactions between these molecules as opposed to hydrophilic cellulose polymers.

DSC results for drug-polymer interactions are typically corroborated and investigated using Fourier Transformed - Infrared Spectroscopy (FTIR), X-Ray Diffraction (XRD) and Nuclear Magnetic Resonance (NMR) [105, 107] studies to identify formation of new bonds or changes in functional groups due to a chemical reaction. Therefore, further investigations would be required to make concrete conclusions.

4.4.4 Mathematical Models of HCT drug release

Various mathematical models were used to understand the release mechanism of HCT from the polymeric matrices. Zero order[108, 109], first order [108], Higuchi [110, 111], Peppas [112, 113] and Hixson-Crowell [114-116] are some common models applicable to existing drug delivery systems. Regression analysis using these models require various assumptions, broadly involving the matrix and drug properties, which are then used to hypothesize the mechanisms involved. Some common drug release mechanisms pertaining to the matrix include swelling, porosity, dissolution and degradation. Additionally, the ratio of drug/polymer and its physicochemical properties such as solubility, ionization and diffusion coefficients can influence the release profile observed for a system [112].

Zero-order kinetics are typically seen with osmotically controlled or reservoir type systems [109] where a membrane can ensure consistent amount of drug release over time. First-order kinetics indicate a concentration gradient-dependent release of drug. This behavior is common in porous systems for hydrophilic drugs since drug diffusion, rather than drug solubility, is a limiting

factor [117]. The Higuchi model was proposed for the quantification of drug release from a planar film of ointment assuming pseudo-steady-state approach. This evolved into an equation with the concentration being directly proportional to the square root of time [111, 118]. The Hixson-Crowell equation, also known as the "cube-root law" takes into account the changes in surface area as the matrix dissolves over time [108]. The Peppas equation, also known as the power-law, was proposed for thin polymeric films with negligible edge effects. It is valid for the first 60% of normalized drug release and the mechanism of drug release can be interpreted from the value of the diffusional exponent, n [119, 120], defined for non-swellable thin films. A value of n=0.5 indicates a Fickian diffusion; n=1 indicates Case-II transport (zero-order) whereas $0.5<n<1$ indicates anomalous transport [118].

However, all these models should not be assessed simply based on correlation values. Peppas et al. demonstrated that Fickian diffusional release from thin polymeric sample where the amount of drug is below its solubility limit is also proportional to square-root of time up to 60% of drug release. This may sometimes be misinterpreted as the Higuchi model and therefore, prior assumptions of the two models must be taken into account before arriving at a conclusion [118]. Table 11 lists the coefficient of determination (R^2) values for the various models tested for comparison.

Table 11: Coefficient of determination values for in vitro release of HCT release models

Formulation	Zero-order	First order	Higuchi	Hixson-Crowell	Peppas* (*n*)	Fickian diffusion*
1.5% K4M	0.5173	0.8731	0.7669	0.9067	0.8947 (0.39)	0.9351
1.5% K4M PLGA	0.5686	0.802	0.7938	0.7289	0.9145 (0.21)	0.8053
0.75% K4M	0.7803	0.986	0.959	0.946	0.9903 (0.40)	0.9876
0.75% K4M PLGA	0.6349	0.8589	0.8278	0.7935	0.9546 (0.15)	0.7899
4% 250L	0.8405	0.9914	0.9819	0.964	0.9924 (0.35)	0.9829
4% 250L PLGA	0.7654	0.9351	0.9479	0.9546	0.9833 (0.35)	0.9769

* Release data up to 60% cumulative release of HCT

Cellulose-based films indicated high R^2 values for first order, Hixson-Crowell, Peppas and Fickian diffusion models. These models supported each other to indicate that the HCT release from micropatterned films was diffusion limited. The *n* values for Peppas equation varied between 0.35 and 0.4 (Table 11) which are lower than the 0.5 value expected for Fickian diffusion. These differences may be due to the swellable nature of the cellulose-based polymers, bidirectional transport and the presence of micropatterns on films [119, 120]. Additionally, the low drug loading of these films do not fulfil the primary requirements of Higuchi model [111, 118], therefore, the R^2 values cannot be truly evaluated for this model.

For films containing HPMC K4M and PLGA, the Peppas model had the highest R^2 values with *n* values between 0.15 and 0.35. The diffusion-limited mechanism is not truly supported by other models and hence, here it might seem that the profiles are pseudo-Fickian [121], wherein the approach to final equilibrium is very slow. For film containing HEC 250L and PLGA, the high R^2 values for all tested models, except zero-order, indicate a diffusion-limited release. This is similar

to its pure cellulose counterpart, 4% 250L, as was also reflected in the similar R^2 values of its cellulose film counterpart.

The lack of a definitive fit for HCT release with various models can be attributed to the complexity of the formulation and processing method. Various cellulose polymers have unique mechanisms of drug release when studied independently. HPC is known to show Fickian behavior in drug release where diffusion is dominant. Alternatively, HEC and HPMC show a combination of drug diffusion and polymer matrix effects [112]. The profiles of drug release in our system would be influenced by a multitude of factors, with each polymer contributing its unique characteristics. The shape and dimensions of our system are different from conventional geometries considered for modelling drug release, such as, cylindrical tablets, spherical granules and slab geometry [119, 120]. The sub-millimeter thickness and additional surface area of micropatterns allows better interaction with the aqueous medium which may improve the wetting rate. The control of release, however, would be impacted by the diffusion of drug through the gel layer and also disintegration of the polymer matrix. Thus, further investigations would be required to characterize the polymeric film matrix and understand the influence of all components within the system on the release of HCT.

4.5 Release of OLO from micropatterned films

4.5.1 Effect of micropattern shape on OLO release

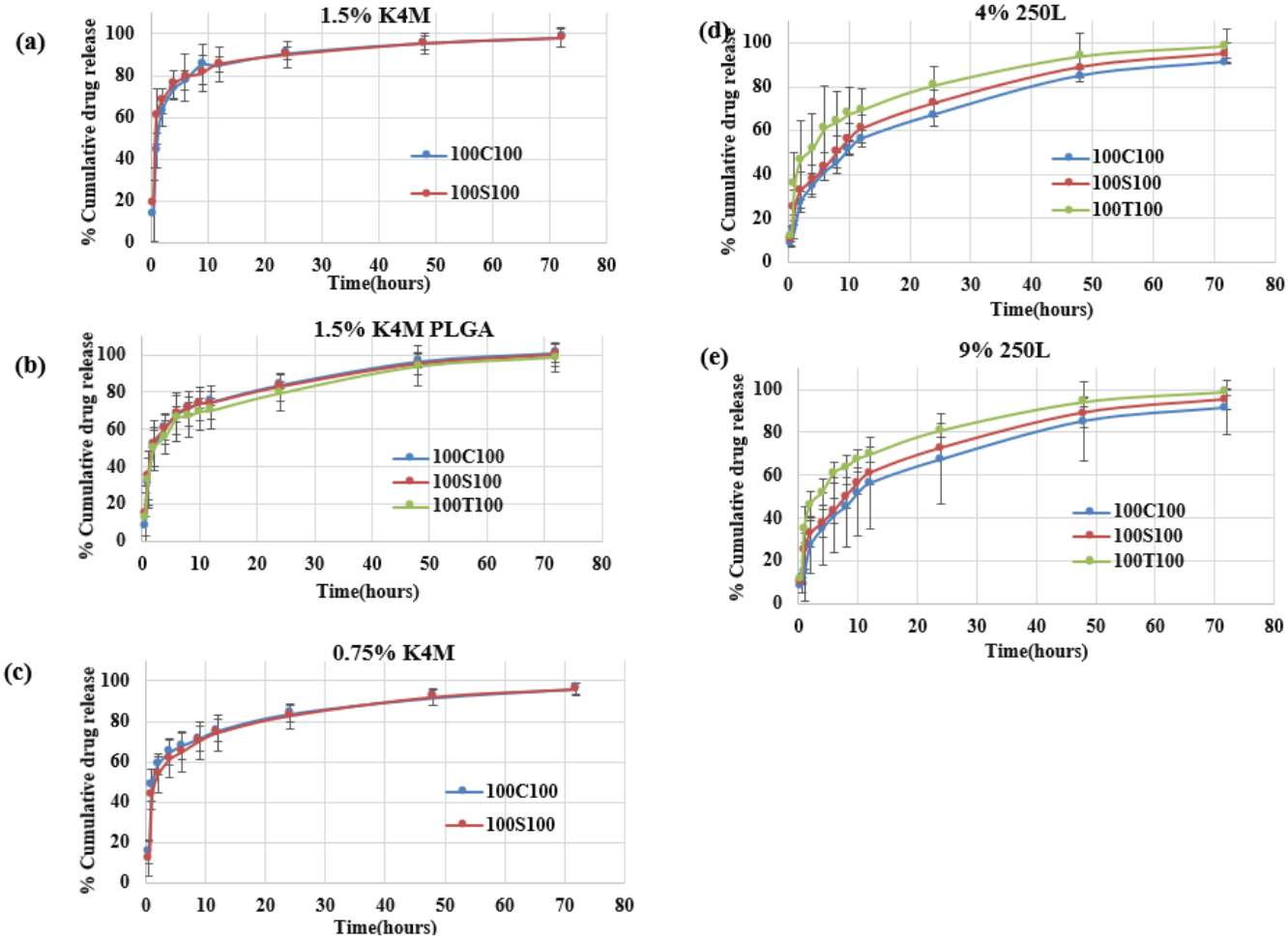

Figure 15: Effect of shape on OLO drug release
Cumulative release of OLO from (a) 1.5% K4M, (b) 1.5% K4M PLGA, (c) 0.75% K4M, (d) 4% 250L, (e) 9% K4M micropatterned films in simulated tear fluid as release media. Data shown is the mean ± standard deviation of three replicates (n=3)

The release profiles of OLO, from films containing circle, square and triangle shaped micropatterns of 100 µm size, are shown in Figure 15. Analysis using RM two-way ANOVA test indicated no significant effect of shape for most formulations, except 4% 250L where the triangle

(100T100) showed faster release compared to circles and squares. Further investigation using Tukey's post hoc test [122] for every time point corroborated with the results of RM two-way ANOVA for all formulations confirming that release was higher for triangles in 4% 250L composition. Since, in general, the micropattern shape did not affect the drug release significantly, the drug release data for different shapes was combined for comparison of OLO formulations in the subsequent sections.

4.5.2 Effect of film composition on OLO release

The release profile of OLO from micropatterned films of various compositions in shown in Figure 16. A high initial burst of at least 45% was observed within 1 hour for 1.5% K4M films as opposed to 1.5% K4M PLGA films with a burst release of around 30%. The PLGA-containing film was found to sustain the release better than the cellulose film until 24 hours, after which both films approached similar OLO release until 72 hours. This may be attributed to the fact that during the preparation of PLGA-containing films, the OLO drug was dispersed with the PLGA phase. The drug that remains associated with the PLGA, will be release slowly due to the water-insoluble nature of PLGA.

The OLO release from 0.75% K4M film was similar to the 1.5% K4M PLGA film. This could be attributed to the fact the 0.75% K4M film composition had low K4M content which was compensated by increasing the concentration of HEC 250L and HPMC E5 equally. This suggests that HEC 250L may have a significant impact on the release of OLO. To investigate the effect of 250L on the release of OLO, compositions with higher 250L content were tested. In case of 4% 250L and 9% 250L films, the initial burst release (~ 30%) and the subsequent release up to 72 hours

was similar. Overall, OLO release was sustained well by higher 250L concentrations up to 48 hours (Figure 16) even though it is a low-viscosity polymer as opposed to K4M. To investigate these observations further, the interaction of OLO with various polymers was studied using DSC.

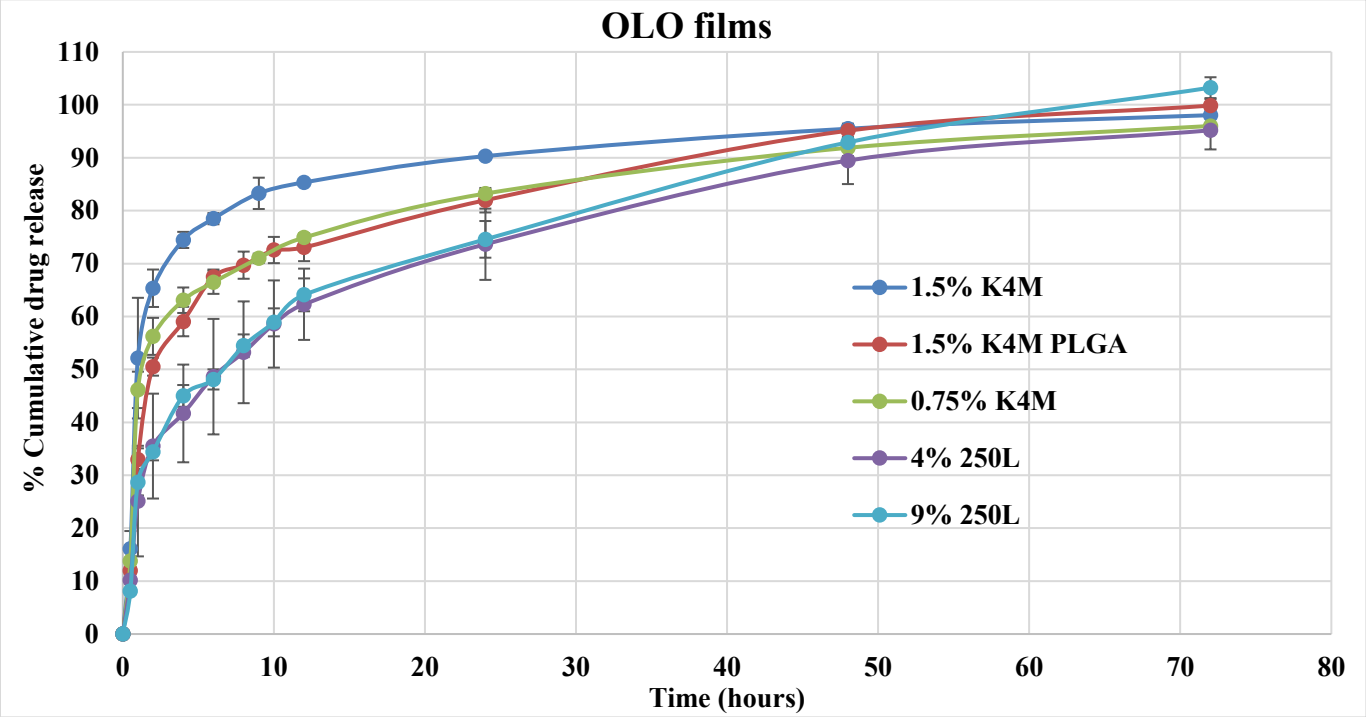

Figure 16: Effect of formulation on OLO release
OLO release from different compositions, 1.5% K4M, 1.5% K4M PLGA, 0.75% K4M, 4% 250L and 9% 250L micropatterned films in simulated tear fluid as release media. Data shown is mean ± standard deviation of three micropattern shapes from each of the three replicates (n=9)

4.5.3 Study of OLO – polymer interaction by DSC

DSC analysis of OLO with individual polymers are shown in Figure 17. DSC of OLO indicated a sharp endothermic peak at 254 °C, typical of a melting point [106]. This endothermic peak shifted in case of 1:1 physical mixture of OLO: PLGA (238 °C) and OLO: HEC (240 °C). These shifts in the peak are indicative of substantial drug-polymer interactions [104, 105, 123].

Endothermic peak shifts observed with other cellulose polymers were similar in intensity and enthalpy.

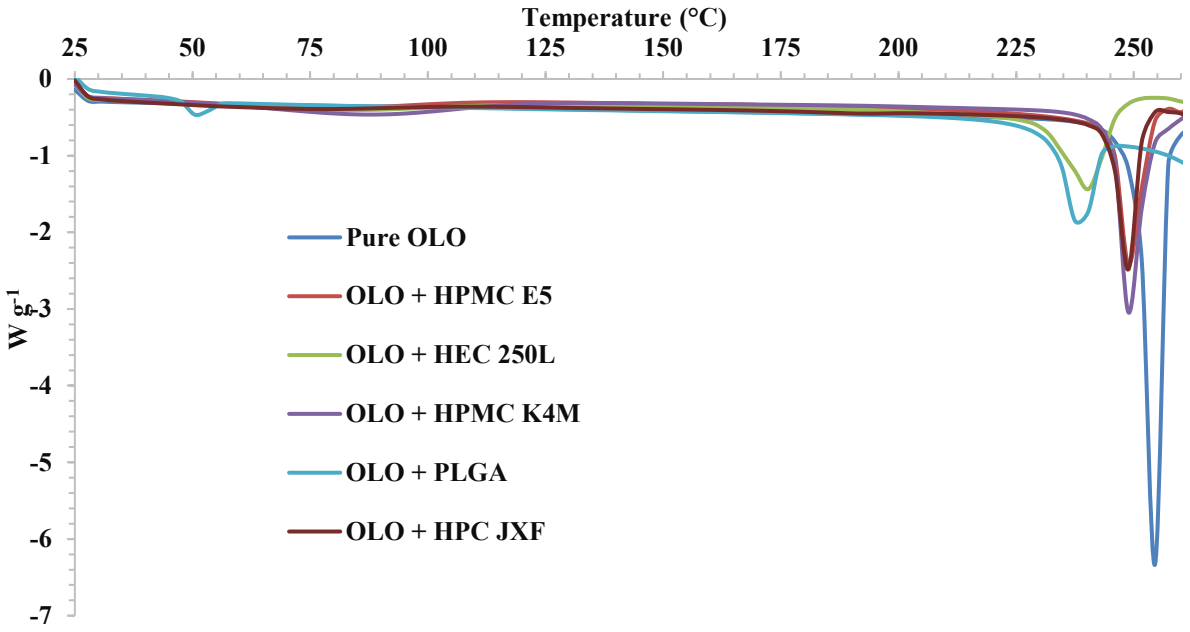

Figure 17: DSC thermograms of OLO and 1:1 physical mixtures of OLO with individual polymers
DSC analysis was carried out by heating samples from 25 – 300 °C at the rate of 10 °C/min. Heat flow data expressed is per gram of sample.

DSC was also performed with polymeric blends representative of the various compositions (Figure 18). Endothermic peak for physical mixtures with 4% 250L and 9% 250L formulations indicated a similar shift, even though the relative polymer compositions were significantly different within these two formulations. The shifts in K4M containing compositions, 1.5% K4M and 0.75% K4M, was also similar. However, the peak shifts in high 250L content compositions (4% 250L and 9% 250L) was significantly greater than the peak shifts in K4M containing compositions (1.5% K4M and 0.75% K4M). This indicated that OLO had greater interactions with HEC 250L as compared to other cellulose-based polymers.

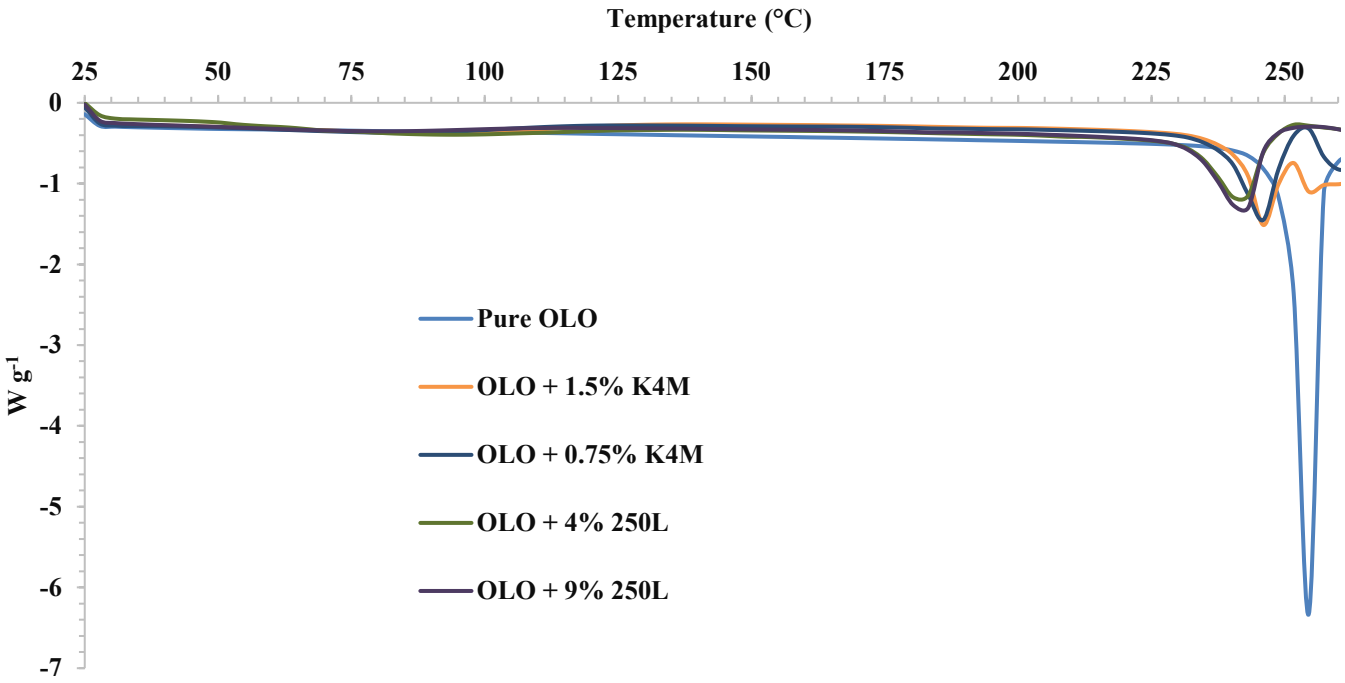

Figure 18: DSC thermograms of OLO and 1:1 physical mixtures of OLO with polymeric blends
DSC analysis was carried out by heating samples from 25 – 300 °C at the rate of 10 °C/min. Heat flow data expressed is per gram of sample.

4.5.4 Mathematical models of OLO release

To understand the release mechanism of OLO from micropatterned films, drug release models discussed in Section 4.4.4 were applied. Table 12 lists the coefficient of determination (R^2) values for the various models tested for comparison of OLO release.

Table 12: Coefficient of determination values for OLO release models

Formulation	Zero-order	First order	Higuchi	Hixson-Crowell	Peppas* (*n*)	Fickian diffusion*
1.5% K4M	0.3651	0.8779	0.6069	0.6644	0.7897 (0.7)	0.9009
1.5% K4M PLGA	0.5241	0.9366	0.7735	0.8869	0.8173 (0.44)	0.9402
0.75% K4M	0.4834	0.9268	0.7197	0.7637	0.7109 (0.32)	0.8889
4% 250L	0.6889	0.9684	0.9055	0.9006	0.9047 (0.46)	0.9632
9% 250L	0.7234	0.9617	0.9216	0.9347	0.8432 (0.49)	0.9433

*Release data up to 60% cumulative release of OLO

For all films, highest R^2 values were observed for Fickian diffusion model, which indicated a primarily diffusion limited drug release. Additionally, films with low K4M (0.75%) or high 250L content (4% 250L and 9% 250L) also demonstrated high R^2 values for first-order release. The rate constants for first order model of 0.75% K4M, 4% 250L and 9% 250L are 0.0366, 0.0393 and 0.05043 hr^{-1}, respectively.

These films, not being more than 300 µm in thickness, allow the aqueous media surrounding them to get imbibed within the hydrophilic polymeric matrix. This is followed by the relaxation polymeric chains to form a gel through which the drug diffuses to the outer media [112]. OLO being a hydrophilic drug, is not limited by local dissolution and travels across the gel layer by virtue of diffusion or concentration gradient limitations. In case of films with high K4M, the gel formed would have a high viscosity indicating a denser network of polymer chains and greater resistance thereby controlling the diffusion of drug molecules from the polymeric matrix. On the other hand, films with low viscosity polymers, do not form as dense networks and the entire hydrated film

would function as a uniform drug reservoir. Therefore, drug release would be limited by difference in concentration gradient of this "drug reservoir" and the surrounding media.

In general, the R^2 values for first order and Fickian diffusion are not significantly different and hence, a single model cannot define the entire system.

4.6 Tensile properties of films

To evaluate the effect of patterns on the mechanical properties of films, tensile testing was carried out on 1.5% K4M and 1.5% K4M PLGA, both representative of cellulose and PLGA films, respectively. The results of tensile strength, Young's modulus and % elongation are shown in **Error! Reference source not found.**. For a given formulation, there was no significant impact of shape on the tensile properties of films. However, tensile strength was found to be significantly dependent on the formulation for micropatterned films. 1.5% K4M films had higher tensile strengths than 1.5% K4M PLGA with significant differences between circle or square cellulose films and PLGA-containing films (Figure 19 (a)). In general, Young's modulus of various cellulose films were found to be higher than PLGA films, although statistically significant for triangle and square micropatterned cellulose films (Figure 19 (b)). This may be attributed to the differences in physicochemical properties of PLGA and cellulose phase. The presence of PLGA might be causing discontinuity in the polymeric chain matrix, hence, affecting its ability to withstand axial tension. The elongation potential was comparable for the two compositions, irrespective of the presence of micropatterns (Figure 19 (c)). All these properties are indicative of mechanical strength of films [124], an important characteristic for the dosage form at the manufacturing and patient use fronts. The film should be able to sustain processes such as peeling and cutting in manufacturing, whereas

the patient should be able to effectively place the insert in the eye. In general, there are no guidelines or defined regulatory ranges for mechanical properties [125]. However, films with moderate tensile strength and low elongation potential are soft and strong, which would be preferable for micropatterned films in order to ensure physical integrity and avoid deformation under shear intensive processes of the eye such as blinking and movement of the eyeball [91].

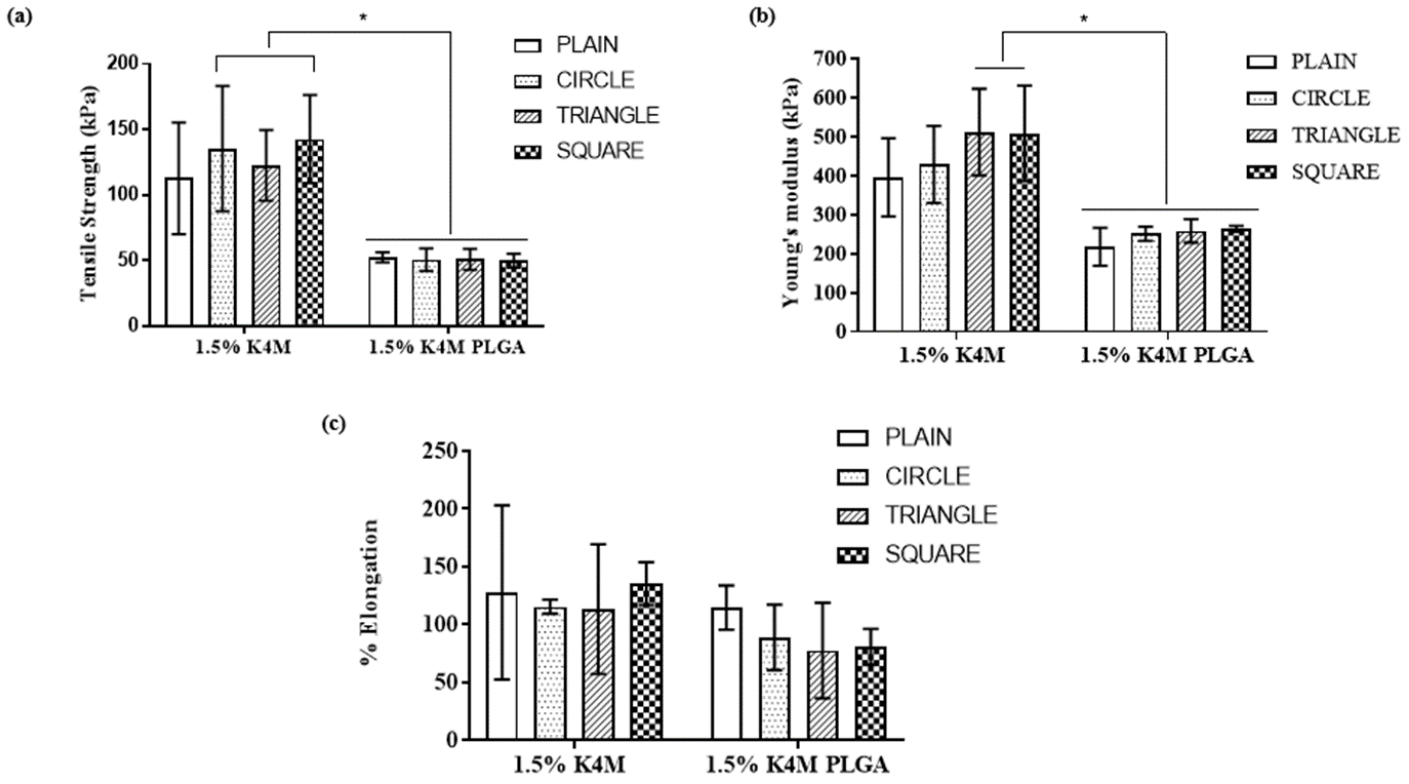

Figure 19: Effect of micropatterns on mechanical properties of placebo films
(a)Tensile strength, (b) Young's modulus and (c) % Elongation of 1.5% K4M and 1.5% K4M PLGA films were evaluated using forces measured by TA.XT texture analyzer. Data presented is mean + standard deviation for three replicates in each group. *$p<0.05$, Two-way ANOVA followed by Tukey's pot hoc test

4.7 Mucoadhesion of micropatterned films

The results from mucoadhesion testing are shown in Figure 20. The films, 1.5% K4M and 1.5% K4M PLGA, were chosen as representative of the cellulose and PLGA films, respectively. The primary aim was to determine whether the presence of micropatterns could resist an external shear better than unpatterned films. The proposed experimental setup (Section 3.2.9) was used to evaluate the work required to move a film over the mucosal tissue surface, under a set of defined parameters. This work could be evaluated as an indirect indication of the extent of adhesion of films to the mucosal surface of the tissue. The force with which the film was allowed to make contact with the tissue, the rate of shear and the distance over which the shear was applied, were chosen to simulate the ocular environment within the limitations of other contributing factors like sensitivity of the instrument, choice of tissue, direction of force measurements.

It was observed that the presence of micropatterns did not significantly improve the mucoadhesion of films to the tissue surface for either composition. One reason could be that compared to the inherent mucoadhesive characteristics of the cellulose polymers in film, the potential effect and contribution of micropatterns is relatively small. Another possibility is the swellable nature of cellulose polymers, which may compromise the physical integrity of micropatterns. Previous work by Yohann Pitale [93] had demonstrated that the work of adhesion was significantly improved by micropatterns as compared to unpatterned film when tested on porcine intestinal tissue. However, the films tested had a high content of Eudragit® polymers, which are more hydrophobic than cellulose polymers and also the loading force used significantly higher (150g as opposed to 10g). Hence, the prominent effect of micropatterns could be a result of these multiple parameters.

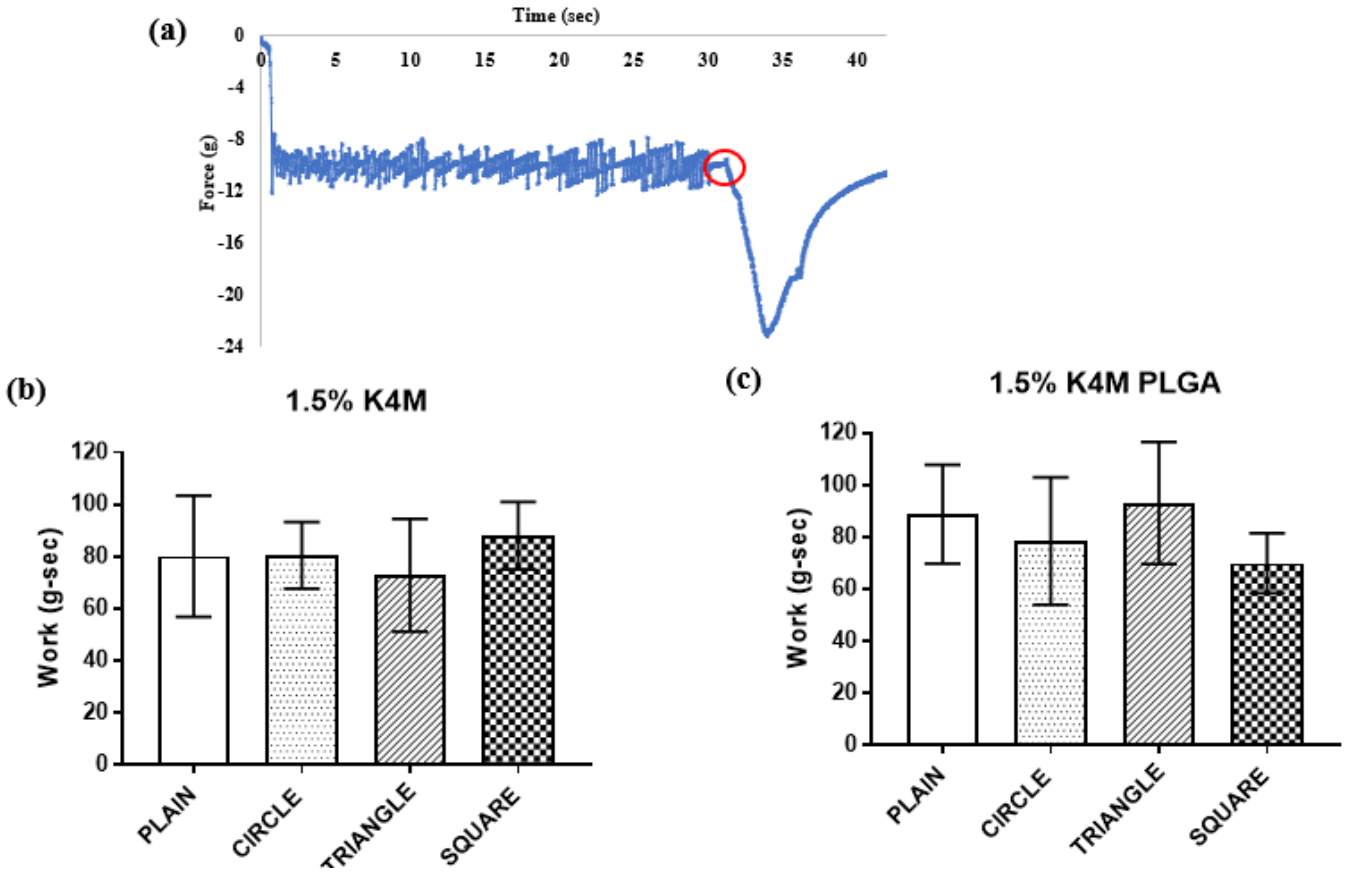

Figure 20: Effect of micropatterns on work of friction
(a) Typical plot of force vs time generated by Exponent software of TA.XT texture analyzer. The beginning of the sliding of porcine tissue is marked in red. Work by friction was evaluated for (b) 1.5% K4M, (c) 1.5% K4M PLGA films by calculating the area under the force-time graph when the porcine tissue was moved horizontally in contact with the micropatterned film sample on probe. Data presented is mean + standard deviation for three replicates in each group.

Another factor that can impact the results of the test is the directionality of tissue movement. Previous studies [68, 69] involved moving the film sample along the axial direction of intestinal tissue, which were relevant within the scope of their endoscopic application. Validation would be required to establish the suitability of using the axial direction of porcine intestinal tissue as a representative of the conjunctival tissue. Tissue variability, mucosal content and the lack of integration of sliding platform with the texture analyzer are other factors that influence the results.

4.8 Conclusion and future directions

Through this study, we demonstrated that polymeric micropatterned films are a versatile platform to incorporate drugs with different physicochemical properties, such as hydrocortisone (water-insoluble) and olopatadine hydrochloride (water-soluble). By using various proportions of GRAS complaint polymers, it was possible to tailor the release of anti-inflammatory drugs for a prolonged period up to 72 hours. Cellulose-based polymers like HPMC K4M, HPMC E5, HEC 250L and HPC JXF were chosen for their various unique properties contributing to the quality of films and the sustenance of drug release. Some common theories of drug release from these water-soluble polymers suggest that the water gets imbibed in the polymeric matrix followed by relaxation of polymeric molecules to form a gel. The viscosity of this gel has the potential to control drug release by virtue of its viscosity and diffusion limiting parameters of the drug molecule. Therefore, a high viscosity polymer, HPMC K4M, was used in our formulations and its effects studied. To further sustain the release of HCT and OLO, PLGA was also incorporated. PLGA has been previously been studied in the form of micro/nano particles and pure PLGA films for ocular applications [31, 78, 79, 102], but we have explored its dispersion in a solid polymeric matrix.

Despite its hydrophobic nature, we could successfully incorporate PLGA in the hydrophilic polymeric matrix but its proportion was limited due to the need of organic solvents like DCM. DCM is a class 2 solvent and the FDA has strict regulations regarding residual solvent content [126]. Also, DCM has a potential to swell PDMS molds used to fabricate films, which might compromise the intended dimensions of micropatterned films.

Micropatterned films of 100 μm sized circles, triangle and squares were fabricated and studied for drug release. These studies indicated a lack of variation for different shapes which may

be due to the large size of patterns and the swellable nature of the polymeric matrix, effectively masking the potential effects of surface area and volume.

Polymeric films containing PLGA maintained physical integrity longer and were able to sustain the release of HCT better than cellulose-based films. DSC studies revealed that HCT had greater interactions with PLGA than other cellulose polymers which may be attributed to their hydrophobic nature. Alternatively, films with high HEC 250L content showed better sustenance in OLO release. This observation was corroborated with the DSC studies which indicated higher interactions of OLO with HEC. However, further investigations with FTIR and XRD studies would be required for both drugs to identify and characterize these potential interactions. The drug release for both HCT and OLO was found to be primarily diffusion limited for all formulations and the lack of a definitive fit for model highlighted the complex nature of these systems. Also, the grade of PLGA used in these studies contains a 50:50 ratio of lactic acid and glycolic acid monomers. Other grades of PLGA have varied capabilities of sustained release based on these ratios. Therefore, future studies would be directed towards exploring the different grades of PLGA and also different drug-loading capacities. The *in vitro* release method used in this work involved the use of release media at physiological pH and in quantities far greater than the biological system of eye. Hence, further optimization studies can be done towards developing a biorelevant system to mimic the tear fluid volume, pH and turnover in the diseased eye.

Tensile studies indicated that micropatterns did not affect the tensile strength of the films. However, the formulation had a significant impact with PLGA-containing films having lower tensile strength than cellulose films which may be attributed to the discontinuity in polymeric chain alignment incurred as PLGA is incorporated in cellulose matrix. PLGA cannot interact as well with the cellulose polymers making the film relatively brittle.

A novel method to evaluate mucoadhesion was developed in an attempt to make the parameters relevant to the ocular conjunctival system. Initial studies indicated that micropatterns did not improve the adhesion of cellulose or PLGA-containing films to the mucosal surface. This may be attributed to the inherent mucoadhesive and swellable properties of cellulose polymers used which may render the effects of micropatterns insignificant. To investigate these, fluorescent dye-loaded micropatterned films can be visualized over the time-course of their placement and compression on the mucosal surface. These studies could also potentially provide insight into an appropriate method of application of the films.

Previous studies with Eudragit-based films and a different method indicated micropatterns significantly improved mucoadhesion [93]. Therefore, further studies would be required to validate the new method using the Eudragit-based film compositions and also check whether the effect of micropatterns on mucoadhesion is formulation dependent. The validated method can then be used to study micropatterns of smaller sizes and their effect on mucoadhesion.

In conclusion, it was demonstrated that the micropatterned polymeric film is a promising platform for prolonged ocular delivery of various drugs and further optimization is required to improve its mucoadhesive properties.

Bibliography

1. American Academy of Opthalmology. *US Eye Disease Statistics*. 2019 [cited 2019 27th February]; Available from: https://www.aao.org/eye-disease-statistics.
2. Opthalmology, A.A.o. *Eye Health Statistics*. 2019 [cited 2019 27th February]; Available from: https://www.aao.org/newsroom/eye-health-statistics.
3. National Eye Institute - National Institute of health, *Eye Disease Statistics*. 2014, NIE-NIH.
4. Gaudana, R., et al., *Ocular drug delivery.* AAPS J, 2010. **12**(3): p. 348-60.
5. Kuno, N. and S. Fujii, *Recent Advances in Ocular Drug Delivery Systems.* Polymers, 2011. **3**(1): p. 193-221.
6. Mishima, S., et al., *Determination of tear volume and tear flow.* Invest Ophthalmol, 1966. **5**(3): p. 264-76.
7. Sosnik, A., J. das Neves, and B. Sarmento, *Mucoadhesive polymers in the design of nano-drug delivery systems for administration by non-parenteral routes: A review.* Progress in Polymer Science, 2014. **39**(12): p. 2030-2075.
8. Hongcheng Zhao, J.E.J., Thomas O. Wood, Marcia M. Jumblatt, *Quantification of MUC5AC Protein in Human Tears.* Cornea, 2001. **20**: p. 873-877.
9. Agrahari, V., et al., *A comprehensive insight on ocular pharmacokinetics.* Drug Deliv Transl Res, 2016. **6**(6): p. 735-754.
10. Saettone, M.F., *Progress and Problems in Ophthalmic Drug Delivery*, in *Business briefing: Pharmatech - Future Drug Delivery*. 2002.
11. Hosoya, K.-i., V.H.L. Lee, and K.-J. Kim, *Roles of the conjunctiva in ocular drug delivery: a review of conjunctival transport mechanisms and their regulation.* European Journal of Pharmaceutics and Biopharmaceutics, 2005. **60**(2): p. 227-240.
12. Thrimawithana, T.R., et al., *Drug delivery to the posterior segment of the eye.* Drug Discovery Today, 2011. **16**(5): p. 270-277.
13. Patel, A., et al., *Ocular drug delivery systems: An overview.* World J Pharmacol, 2013. **2**(2): p. 47-64.
14. Chen, H., et al., *Recent Developments in Ophthalmic Drug Delivery Systems for Therapy of Both Anterior and Posterior Segment Diseases.* Colloid and Interface Science Communications, 2018. **24**: p. 54-61.
15. Molokhia, S.A., et al., *Anterior eye segment drug delivery systems: current treatments and future challenges.* J Ocul Pharmacol Ther, 2013. **29**(2): p. 92-105.
16. Xu, J., et al., *A comprehensive review on contact lens for ophthalmic drug delivery.* J Control Release, 2018. **281**: p. 97-118.
17. Rawas-Qalaji, M. and C.A. Williams, *Advances in ocular drug delivery.* Curr Eye Res, 2012. **37**(5): p. 345-56.
18. Sklubalova, Z. and Z. Zatloukal, *Study of eye drops dispensing and dose variability by using plastic dropper tips.* Drug Dev Ind Pharm, 2006. **32**(2): p. 197-205.
19. Diestelhorst, M., K.-A. Kwon, and R. Süverkrup, *Dose uniformity of ophthalmic suspensions.* Journal of Cataract & Refractive Surgery, 1998. **24**(5): p. 672-677.

20. Taylor, S.A., S.M. Galbraith, and R.P. Mills, *Causes Of Non-Compliance With Drug Regimens In Glaucoma Patients: A Qualitative Study.* Journal of Ocular Pharmacology and Therapeutics, 2002. **18**(5): p. 401-409.
21. Tsai, J.C.M., Cori A. ; Ramos, Sarah E. ; Schlundt, David G.; Pichert, James W. , *Compliance Barriers in Glaucoma.* Journal of Glaucoma, 2013. **12**(5): p. 393-398.
22. Hermann, M.M., C. Üstündag, and M. Diestelhorst, *Electronic compliance monitoring of topical treatment after ophthalmic surgery.* International Ophthalmology, 2010. **30**(4): p. 385-390.
23. Olthoff, C.M.G., et al., *Noncompliance with Ocular Hypotensive Treatment in Patients with Glaucoma or Ocular Hypertension: An Evidence-Based Review.* Ophthalmology, 2005. **112**(6): p. 953-961.e7.
24. Conway, B.R., *Recent patents on ocular drug delivery systems.* Recent Pat Drug Deliv Formul, 2008. **2**(1): p. 1-8.
25. Morrison, P.W. and V.V. Khutoryanskiy, *Advances in ophthalmic drug delivery.* Ther Deliv, 2014. **5**(12): p. 1297-315.
26. Loftssona, T. and T. Järvinen, *Cyclodextrins in ophthalmic drug delivery.* Advanced Drug Delivery Reviews, 1999. **36**(1): p. 59-79.
27. Gaudana, R., et al., *Recent perspectives in ocular drug delivery.* Pharm Res, 2009. **26**(5): p. 1197-216.
28. Baspinar, Y., et al., *Corneal permeation studies of everolimus microemulsion.* J Ocul Pharmacol Ther, 2008. **24**(4): p. 399-402.
29. Muchtar, S., et al., *Ex-vivo permeation study of indomethacin from a submicron emulsion through albino rabbit cornea.* Journal of Controlled Release, 1997. **44**(1): p. 55-64.
30. Nagarwal, R.C., et al., *Polymeric nanoparticulate system: A potential approach for ocular drug delivery.* Journal of Controlled Release, 2009. **136**(1): p. 2-13.
31. Gavini, E., et al., *PLGA microspheres for the ocular delivery of a peptide drug, vancomycin using emulsification/spray-drying as the preparation method: in vitro/in vivo studies.* European Journal of Pharmaceutics and Biopharmaceutics, 2004. **57**(2): p. 207-212.
32. Raymond A. Huml, C.R., Kamali Chance, *Key Challenges to US Topical Ocular Drug Development.* Regulatory Focus, 2009: p. 47-52.
33. Khutoryanskiy, V.V., *Advances in mucoadhesion and mucoadhesive polymers.* Macromol Biosci, 2011. **11**(6): p. 748-64.
34. Shaikh, R., et al., *Mucoadhesive drug delivery systems.* J Pharm Bioallied Sci, 2011. **3**(1): p. 89-100.
35. Yu, T., G.P. Andrews, and D.S. Jones, *Mucoadhesion and Characterization of Mucoadhesive Properties*, in *Mucosal Delivery of Biopharmaceuticals*. 2014. p. 35-58.
36. Ludwig, A., *The use of mucoadhesive polymers in ocular drug delivery.* Adv Drug Deliv Rev, 2005. **57**(11): p. 1595-639.
37. Marner, K., et al., *Viscous Carbomer eye drops in patients with dry eye*. Vol. 74. 2009. 249-252.
38. Calles, J.A., et al., *Polymers in Ophthalmology*, in *Advanced Polymers in Medicine*. 2015. p. 147-176.
39. U.S. Food and Drug Administration. *Orange Book: Approved Drug Products with Therapeutic Equivalence Evaluations*. 2019 [cited 2019 12th March]; Available from: https://www.accessdata.fda.gov/Scripts/cder/ob/search_product.cfm.

40. Brennan, N.A., et al., *A 1-year prospective clinical trial of balafilcon a (purevision) silicone-hydrogel contact lenses used on a 30-day continuous wear schedule.* Ophthalmology, 2002. **109**(6): p. 1172-1177.
41. Jain, M.R. and V. Batra, *Steroid penetration in human aqueous with 'Sauflon 70' lenses.* Indian Journal of Ophthalmology, 1979. **27**(2): p. 26-31.
42. Carreira, A.S., et al., *New drug-eluting lenses to be applied as bandages after keratoprosthesis implantation.* Int J Pharm, 2014. **477**(1-2): p. 218-26.
43. Than, A., et al., *Self-implantable double-layered micro-drug-reservoirs for efficient and controlled ocular drug delivery.* Nat Commun, 2018. **9**(1): p. 4433.
44. Jiang, J., et al., *Coated microneedles for drug delivery to the eye.* Invest Ophthalmol Vis Sci, 2007. **48**(9): p. 4038-43.
45. Thakur, R.R., et al., *Rapidly dissolving polymeric microneedles for minimally invasive intraocular drug delivery.* Drug Deliv Transl Res, 2016. **6**(6): p. 800-815.
46. Than, A., et al., *Self-implantable double-layered micro-drug-reservoirs for efficient and controlled ocular drug delivery.* Nature Communications, 2018. **9**(1): p. 4433.
47. Gittard, S.D., et al., *The Effects of Geometry on Skin Penetration and Failure of Polymer Microneedles.* J Adhes Sci Technol, 2013. **27**(3): p. 227-243.
48. Karki, S., et al., *Thin films as an emerging platform for drug delivery.* Asian Journal of Pharmaceutical Sciences, 2016. **11**(5): p. 559-574.
49. Baeyens, V., et al., *Clinical evaluation of bioadhesive ophthalmic drug inserts (BODI®) for the treatment of external ocular infections in dogs.* Journal of Controlled Release, 2002. **85**(1): p. 163-168.
50. Watsky, M.A., M.M. Jablonski, and H.F. Edelhauser, *Comparison of conjunctival and corneal surface areas in rabbit and human.* Curr Eye Res, 1988. **7**(5): p. 483-6.
51. Aburahma, M.H. and A.A. Mahmoud, *Biodegradable Ocular Inserts for Sustained Delivery of Brimonidine Tartarate: Preparation and In Vitro/In Vivo Evaluation.* AAPS PharmSciTech, 2011. **12**(4): p. 1335-1347.
52. Karthikeyan, D., et al., *The concept of ocular inserts as drug delivery systems: An overview.* Asian Journal of Pharmaceutics, 2008. **2**(4).
53. Li, Z., et al., *The Effect of Air Pollution on the Occurrence of Nonspecific Conjunctivitis.* Journal of ophthalmology, 2016. **2016**: p. 3628762-3628762.
54. Sayin, N., N. Kara, and G. Pekel, *Ocular complications of diabetes mellitus.* World journal of diabetes, 2015. **6**(1): p. 92-108.
55. Hong, J., et al., *Ambient air pollution, weather changes, and outpatient visits for allergic conjunctivitis: A retrospective registry study.* Scientific reports, 2016. **6**: p. 23858-23858.
56. Carr, W., J. Schaeffer, and E. Donnenfeld, *Treating allergic conjunctivitis: A once-daily medication that provides 24-hour symptom relief.* Allergy & rhinology (Providence, R.I.), 2016. **7**(2): p. 107-114.
57. La Rosa, M., et al., *Allergic conjunctivitis: a comprehensive review of the literature.* Italian journal of pediatrics, 2013. **39**: p. 18-18.
58. Aptel, F., et al., *Management of postoperative inflammation after cataract and complex ocular surgeries: a systematic review and Delphi survey.* British Journal of Ophthalmology, 2017. **101**(11): p. 1451.
59. Erdinest, N. and A. Solomon, *Topical immunomodulators in the management of allergic eye diseases.* Curr Opin Allergy Clin Immunol, 2014. **14**(5): p. 457-63.

60. Mueller, J.B. and C.M. McStay, *Ocular infection and inflammation.* Emerg Med Clin North Am, 2008. **26**(1): p. 57-72, vi.
61. Hindman, H.B., S.B. Patel, and A.S. Jun, *Rationale for Adjunctive Topical Corticosteroids in Bacterial Keratitis.* Archives of Ophthalmology, 2009. **127**(1): p. 97-102.
62. Ron Melton, R.T., Patrick Vollmer, *2017 Clinical Guide To Ophthalmic Drugs*, in *Review of Optometry*. 2017.
63. Autumn, K., et al., *Adhesive force of a single gecko foot-hair.* Nature, 2000. **405**: p. 681.
64. Liu, K., et al., *Superhydrophobic gecko feet with high adhesive forces towards water and their bio-inspired materials.* Nanoscale, 2012. **4**(3): p. 768-72.
65. Mahdavi, A., et al., *A biodegradable and biocompatible gecko-inspired tissue adhesive.* Proc Natl Acad Sci U S A, 2008. **105**(7): p. 2307-12.
66. William Bertolino, L.E.F., Claire M McLeod, Andrea Lai, Sandra Lam, Shannon Taylor *Anti-migration micropatterned stent coating*, USPTO, Editor. 2016: USA.
67. Sean P. Fleury, M.D.W., Dane T. Seddon,Laura Elizabeth Firstenberg,Paul Smith,Gary J. Leanna,Claude O. Clerc,James Weldon,Steven E. Walak *Superhydrophobic coating for airway mucus plugging prevention*. 2017, Boston Scientific Scimed Inc.
68. Glass, P., E. Cheung, and M. Sitti*, *A Legged Anchoring Mechanism for Capsule Endoscopes Using Micropatterned Adhesives.* IEEE Transactions on Biomedical Engineering, 2008. **55**(12): p. 2759-2767.
69. Zhang, H., et al., *Friction Enhancement between Microscopically Patterned Polydimethylsiloxane and Rabbit Small Intestinal Tract Based on Different Lubrication Mechanisms.* ACS Biomaterials Science & Engineering, 2016. **2**(6): p. 900-907.
70. Attre, R. and H.S. Dua, *Treatment of Post-operative Inflammation following Cataract Surgery – A Review.* European Ophthalmic Review, 2012. **06**(02).
71. Korenfeld, M.S., et al., *Difluprednate ophthalmic emulsion 0.05% for postoperative inflammation and pain.* Journal of Cataract & Refractive Surgery, 2009. **35**(1): p. 26-34.
72. Pleyer, U., P.G. Ursell, and P. Rama, *Intraocular pressure effects of common topical steroids for post-cataract inflammation: are they all the same?* Ophthalmology and therapy, 2013. **2**(2): p. 55-72.
73. National Center for Biotechnology Information. *PubChem Compound Database; CID=5754*. 2019 Mar 10, 2019]; Available from: https://pubchem.ncbi.nlm.nih.gov/compound/5754.
74. National Center for Biotechnology Information, *PubChem Substance Database; SID=329818840.* 2019.
75. Alcon Laboratories, I., *LABEL: PAZEO - olopatadine hydrochloride solution* N.U.S.L.o. Medicine, Editor. 2018.
76. U.S. Food and Drug Administration, *Ophthalmic drug products for over-the-counter human use*, D.o.H.a.H. Services, Editor. 2018, Government Publishing Office.
77. Harmonization, I.C.f., *ICH Q3C-R7_Document_Guideline_2018_1015*, I.C.f. Harmonization, Editor.
78. Makadia, H.K. and S.J. Siegel, *Poly Lactic-co-Glycolic Acid (PLGA) as Biodegradable Controlled Drug Delivery Carrier.* Polymers (Basel), 2011. **3**(3): p. 1377-1397.
79. Salama, A.H., A.A. Mahmoud, and R. Kamel, *A Novel Method for Preparing Surface-Modified Fluocinolone Acetonide Loaded PLGA Nanoparticles for Ocular Use: In Vitro and In Vivo Evaluations.* AAPS PharmSciTech, 2016. **17**(5): p. 1159-1172.

80. Magdalena Stevanovi, D.U., *Polylactide-co-glycolide-based Micro and Nanoparticles for the Controlled Drug Delivery of Vitamins.* Current Nanoscience, 2009. **5**.
81. Ito, F., H. Fujimori, and K. Makino, *Incorporation of water-soluble drugs in PLGA microspheres.* Colloids Surf B Biointerfaces, 2007. **54**(2): p. 173-8.
82. Morales, J.O. and J.T. McConville, *Manufacture and characterization of mucoadhesive buccal films.* Eur J Pharm Biopharm, 2011. **77**(2): p. 187-99.
83. Colorcon, *General Properties of METHOCEL™, Premium Cellulose Ethers.* 2019.
84. Dow Chemical Company, *METHOCEL Cellulose Ethers in Aqueous Systems for Tablet Coating*. 2002.
85. Nguyen, T. and R. Latkany, *Review of hydroxypropyl cellulose ophthalmic inserts for treatment of dry eye.* Clin Ophthalmol, 2011. **5**: p. 587-91.
86. Borges, A.F., et al., *Oral films: Current status and future perspectives: I — Galenical development and quality attributes.* Journal of Controlled Release, 2015. **206**: p. 1-19.
87. Thomas m. Reilly, S.B.T., Galia T. Krayz, *Applications of Complementary Polymers in HPMC Hydrophilic Extended Release Matrices.* Drug Delivery Technology, 2009. **9**.
88. Ashland, *Formulating elegant liquid and semisolid drug products*. 2018.
89. Ashland, *Klucel™ hydroxypropylcellulose - Physical and chemical properties*. 2017.
90. Ishida, W., et al., *Conjunctival macrophages act as antigen-presenting cells in the conjunctiva during the development of experimental allergic conjunctivitis.* Molecular vision, 2010. **16**: p. 1280-1285.
91. Mathurm, M. and R.M. Gilhotra, *Glycerogelatin-based ocular inserts of aceclofenac: physicochemical, drug release studies and efficacy against prostaglandin E(2)-induced ocular inflammation.* Drug Deliv, 2011. **18**(1): p. 54-64.
92. Lee, J.W., J.H. Park, and M.R. Prausnitz, *Dissolving microneedles for transdermal drug delivery.* Biomaterials, 2008. **29**(13): p. 2113-24.
93. Pitale, Y.A., *Polymeric micropatterned films: A platform for enhanced mucoadhesion*, in *Department of Pharmaceutical Sciences, School of Pharmacy*. 2017, University of Pittsburgh Pittsburgh, PA.
94. Friend, J. and L. Yeo, *Fabrication of microfluidic devices using polydimethylsiloxane.* Biomicrofluidics, 2010. **4**(2): p. 026502.
95. Bettinger, C.J., et al., *Silk Fibroin Microfluidic Devices.* Advanced materials (Deerfield Beach, Fla.), 2007. **19**(5): p. 2847-2850.
96. Zhao, X.M., Y.N. Xia, and G.M. Whitesides, *Fabrication of three-dimensional micro-structures: Microtransfer molding.* Advanced Materials, 1996. **8**(10): p. 837-&.
97. Lee, J.N., C. Park, and G.M. Whitesides, *Solvent Compatibility of Poly(dimethylsiloxane)-Based Microfluidic Devices.* Analytical Chemistry, 2003. **75**(23): p. 6544-6554.
98. Marques, M.R.C., R. Loebenberg, and M. Almukainzi, *Simulated Biological Fluids with Possible Application in Dissolution Testing.* Dissolution Technologies, 2011. **18**(3): p. 15-28.
99. Jae-Seob Kwak, T.-W.K., *A Review of Adhesion and Friction Models for Gecko Feet.* International journal of precision engineering and manufacturing 2010. **11**(1): p. 171-186.
100. Fiebrig, I., D. Ss, and S. Harding, *Methods used to develop mucoadhesive drug delivery systems: bioadhesion in the gastrointestinal tract*, in *Biopolymer Mixtures*. 1995, Nottingham University Press.
101. Molladavoodi, S., et al., *Corneal epithelial cells exposed to shear stress show altered cytoskeleton and migratory behaviour.* PLoS One, 2017. **12**(6): p. e0178981.

102. Klose, D., et al., *PLGA-based drug delivery systems: importance of the type of drug and device geometry.* Int J Pharm, 2008. **354**(1-2): p. 95-103.
103. GraphPad Software. *Point of confusion: ANOVA with a quantitative factor*. 2018 [cited 2019 14th februray]; Available from: https://www.graphpad.com/guides/prism/7/statistics/index.htm?overuse_of_repeated_measures_t.htm.
104. Wong, T.W., et al., *Design of controlled-release solid dosage forms of alginate and chitosan using microwave.* Journal of Controlled Release, 2002. **84**(3): p. 99-114.
105. Kumar, N., et al., *Thermal characterization and compatibility studies of itraconazole and excipients for development of solid lipid nanoparticles.* Journal of Thermal Analysis and Calorimetry, 2013. **115**(3): p. 2375-2383.
106. Bhadeshia, H.K.D.H. *Differential Scanning Calorimetry*. 2002 [cited 2019 16th March]; Available from: https://www.phase-trans.msm.cam.ac.uk/2002/Thermal2.pdf.
107. Puttipipatkhachorn, S., et al., *Drug physical state and drug–polymer interaction on drug release from chitosan matrix films.* Journal of Controlled Release, 2001. **75**(1): p. 143-153.
108. Siepmann, J. and F. Siepmann, *Mathematical modeling of drug dissolution.* Int J Pharm, 2013. **453**(1): p. 12-24.
109. Peppas, N.A. and B. Narasimhan, *Mathematical models in drug delivery: How modeling has shaped the way we design new drug delivery systems.* Journal of Controlled Release, 2014. **190**: p. 75-81.
110. Higuchi, T., *Mechanism of sustained-action medication. Theoretical analysis of rate of release of solid drugs dispersed in solid matrices.* Journal of Pharmaceutical Sciences, 1963. **52**(12): p. 1145-1149.
111. Higuchi, T., *Rate of Release of Medicaments from Ointment Bases Containing Drugs in Suspension.* Journal of Pharmaceutical Sciences, 1961. **50**(10): p. 874-875.
112. Maderuelo, C., A. Zarzuelo, and J.M. Lanao, *Critical factors in the release of drugs from sustained release hydrophilic matrices.* J Control Release, 2011. **154**(1): p. 2-19.
113. Korsmeyer, R.W. and N.A. Peppas, *Effect of the morphology of hydrophilic polymeric matrices on the diffusion and release of water soluble drugs.* Journal of Membrane Science, 1981. **9**(3): p. 211-227.
114. Hixson, A.W. and J.H. Crowell, *Dependence of Reaction Velocity upon surface and Agitation. I. Theoretical consideration.* Industrial & Engineering Chemistry, 1931. **23**(8): p. 923-931.
115. Hixson, A.W. and J.H. Crowell, *Dependence of Reaction Velocity upon surface and Agitation. III. Experimental procedure in study of agitation.* Industrial & Engineering Chemistry, 1931. **23**(9): p. 1002-1009.
116. Hixson, A.W. and J.H. Crowell, *Dependence of Reaction Velocity upon Surface and Agitation. II. Experimental procedure in study of surface.* Industrial & Engineering Chemistry, 1931. **23**(10): p. 1160-1168.
117. Dash, S., et al., *Kinetic modeling on drug release from controlled drug delivery systems.* Acta Pol Pharm, 2010. **67**(3): p. 217-23.
118. Siepmann, J. and N.A. Peppas, *Higuchi equation: derivation, applications, use and misuse.* Int J Pharm, 2011. **418**(1): p. 6-12.
119. Ritger, P.L. and N.A. Peppas, *A simple equation for description of solute release I. Fickian and non-fickian release from non-swellable devices in the form of slabs, spheres, cylinders or discs.* Journal of Controlled Release, 1987. **5**(1): p. 23-36.

120. Ritger, P.L. and N.A. Peppas, *A simple equation for description of solute release II. Fickian and anomalous release from swellable devices.* Journal of Controlled Release, 1987. **5**(1): p. 37-42.
121. Song, F., et al., *Genipin-crosslinked casein hydrogels for controlled drug delivery.* International Journal of Pharmaceutics, 2009. **373**(1): p. 41-47.
122. GraphPad Software. *Tukey and Dunnett tests in Prism*. 2019 [cited 2019 14th March]; Available from: https://www.graphpad.com/guides/prism/7/statistics/index.htm?stat_the_methods_of_tukey_and_dunne.htm.
123. Li, L., E. Liu, and C.H. Lim, *Micro-DSC and Rheological Studies of Interactions between Methylcellulose and Surfactants.* The Journal of Physical Chemistry B, 2007. **111**(23): p. 6410-6416.
124. Zhang, W., et al., *Development of a vaginal delivery film containing EFdA, a novel anti-HIV nucleoside reverse transcriptase inhibitor.* Int J Pharm, 2014. **461**(1-2): p. 203-13.
125. Abdelkader, H., B. Pierscionek, and R.G. Alany, *Novel in situ gelling ocular films for the opioid growth factor-receptor antagonist-naltrexone hydrochloride: Fabrication, mechanical properties, mucoadhesion, tolerability and stability studies.* International Journal of Pharmaceutics, 2014. **477**(1): p. 631-642.
126. U.S. Food and Drug Administration, *Appendix 5. Toxicological data for class 2 solvents*, U.S.F.a.D. Administration, Editor. p. 1-87.